Environment International 155 (2021) 106688

Contents lists available at ScienceDirect

Environment International

journal homepage: www.elsevier.com/locate/envint

Potential health risks due to in-car aerosol exposure across ten global cities

Prashant Kumar [a,b,*], Sarkawt Hama [a], Rana Alaa Abbass [a], Thiago Nogueira [a,c,d], Veronika S. Brand [a,d], K.V. Abhijith [a], Maria de Fatima Andrade [d], Araya Asfaw [e], Kosar Hama Aziz [f], Shi-Jie Cao [a,g], Ahmed El-Gendy [h], Mukesh Khare [i], Adamson S. Muula [j,o], S.M. Shiva Nagendra [k], Aiwerasia Vera Ngowi [l], Khalid Omer [f], Yris Olaya [m], Abdus Salam [n]

[a] Global Centre for Clean Air Research (GCARE), Department of Civil and Environmental Engineering, Faculty of Engineering and Physical Sciences, University of Surrey, Guildford GU2 7XH, Surrey, United Kingdom
[b] Department of Civil, Structural & Environmental Engineering, Trinity College Dublin, Dublin, Ireland
[c] Departamento de Saúde Ambiental – Faculdade de Saúde Pública, Universidade de São Paulo, São Paulo, Brazil
[d] Departamento de Ciências Atmosféricas – Instituto de Astronomia, Geofísica e Ciências Atmosféricas— IAG, Universidade de São Paulo, São Paulo, Brazil
[e] Physics Department, Addis Ababa University, Ethiopia
[f] Department of Chemistry, College of Science, University of Sulaimani, Kurdistan Region, Iraq
[g] School of Architecture, Southeast University, Nanjing 210096, China
[h] Department of Construction Engineering, School of Sciences and Engineering, The American University in Cairo, New Cairo 11835, Egypt
[i] Department of Civil Engineering, Indian Institute of Technology Delhi, India
[j] University of Malawi, Malawi
[k] Department of Civil Engineering, Indian Institute of Technology Madras, India
[l] Department of Environmental and Occupational Health, Muhimbili University of Health and Allied Sciences, Dar-es-Salaam, Tanzania
[m] Departamento de Ciencias de la Computación y la Decisión, Universidad Nacional de Colombia, Sede Medellín, Colombia
[n] Department of Chemistry, Faculty of Science, University of Dhaka, Bangladesh, Dhaka 1000, Bangladesh
[o] Kamuzu University of Health Sciences, Blantyre, Malawi

ARTICLE INFO

Handling Editor: Qi-Hong Deng

Keywords:
$PM_{2.5}$
In-car aerosol exposure
Potential health risks
Hotspots
Inhaled doses
CArE-cities project

ABSTRACT

Car microenvironments significantly contribute to the daily pollution exposure of commuters, yet health and socioeconomic studies focused on in-car exposure are rare. This study aims to assess the relationship between air pollution levels and socioeconomic indicators (fuel prices, city-specific GDP, road density, the value of statistical life (VSL), health burden and economic losses resulting from exposure to fine particulate matter ≤2.5 μm; $PM_{2.5}$) during car journeys in ten cities: Dhaka (Bangladesh); Chennai (India); Guangzhou (China); Medellín (Colombia); São Paulo (Brazil); Cairo (Egypt); Sulaymaniyah (Iraq); Addis Ababa (Ethiopia); Blantyre (Malawi); and Dar-es-Salaam (Tanzania). Data collected by portable laser particle counters were used to develop a proxy of car-user exposure profiles. Hotspots on all city routes displayed higher $PM_{2.5}$ concentrations and disproportionately high inhaled doses. For instance, the time spent at the hotspots in Guangzhou and Addis Ababa was 26% and 28% of total trip time, but corresponded to 54% and 56%, respectively, of the total $PM_{2.5}$ inhaled dose. With the exception of Guangzhou, all the cities showed a decrease in per cent length of hotspots with an increase in GDP and VSL. Exposure levels were independent of fuel prices in most cities. The largest health burden related to in-car $PM_{2.5}$ exposure was estimated for Dar-es-Salam (81.6 ± 39.3 μg m^{-3}), Blantyre (82.9 ± 44.0) and Dhaka (62.3 ± 32.0) with deaths per 100,000 of the car commuting population per year of 2.46 (2.28–2.63), 1.11 (0.97–1.26) and 1.10 (1.05–1.15), respectively. However, the modest health burden of 0.07 (0.06–0.08), 0.10 (0.09–0.12) and 0.02 (0.02–0.03) deaths per 100,000 of the car commuting population per year were estimated for Medellin (23 ± 13.7 μg m^{-3}), São Paulo (25.6 ± 11.7) and Sulaymaniyah (22.4 ± 15.0), respectively. Lower GDP was found to be associated with higher economic losses due to health burdens caused by air pollution in most cities, indicating a socioeconomic discrepancy. This assessment of health and socioeconomic parameters associated with in-car $PM_{2.5}$ exposure highlights the importance of implementing plausible solutions to make a positive impact on peoples' lives in these cities.

* Corresponding author at: Global Centre for Clean Air Research (GCARE), Department of Civil and Environmental Engineering, Faculty of Engineering and Physical Sciences, University of Surrey, Guildford GU2 7XH, United Kingdom.
E-mail address: p.kumar@surrey.ac.uk (P. Kumar).

https://doi.org/10.1016/j.envint.2021.106688
Received 18 January 2021; Received in revised form 26 April 2021; Accepted 31 May 2021
Available online 15 June 2021

1. Introduction

Exposure to airborne fine particulate matter is amongst the top ten environmental health risk factors globally (GBD, 2019). $PM_{2.5}$ exposure is a function of the concentration of pollutants and the time spent by individuals in any microenvironment (Bigazzi and Figliozzi, 2014; Kumar et al., 2018). Commuters are exposed to high levels of pollutants (de Nazelle et al., 2012), which often do not meet air quality standards. Here, we analysed first-hand datasets of $PM_{2.5}$ concentrations measured in-car during commuting in ten global cities to provide unique insights in relation to excessive $PM_{2.5}$ exposure, traffic conditions, fuel prices, health burden and economic losses. Mitigation strategies were developed that meet inter-related Sustainable Development Goals (UN, 2018): Good health (SDG3), Clean energy (SDG7), and Sustainable cities (SDG11). By studying in-car aerosol exposure in a range of different cities, effective air pollution mitigation measures and best practice guidance may be developed including, using electric buses, public transport and active urban mobility.

Commuters' exposure to concentrations of traffic-related air pollutants (TRAP) can be 3–10 times greater than their exposure to background pollutants (Krzyzanowski et al., 2005). The high concentrations of TRAP tend to accumulate near, or on, roads (Kumar et al., 2021; Leavey et al., 2017), with the highest exposure zones identified within 200–300 m of busy roads and highways (HEI, 2010; Goel and Kumar, 2015). Exposure levels to TRAP in transport microenvironments are related to factors such as time and activity patterns, travel mode, vehicle settings, ambient pollutant concentrations, traffic density, road characteristics, and meteorological conditions (Rivas et al., 2017; Bauer et al., 2018; Kolluru et al., 2018). It is important to identify individual TRAP contributions from different transport microenvironments to enable accurate and effective information to be obtained for reducing respective personal exposure.

Within cities, areas with higher pollutant levels than their surroundings are known as "hotspots". Hotspots are usually characterised by large spatial and temporal concentration gradients and people working or living in these zones have the possibility of being exposed to elevated air pollution levels. Therefore, it is vital to understand the spatio-temporal distribution of exposure levels in road hotspots to carry out a comprehensive risk assessment that can consider both actual and representative exposure levels. The distribution of air pollutants has been found to be inequitable, with people living in most deprived areas generally suffering from high levels of exposure (Richardson et al., 2013, Yu and Stuart, 2016). The associations between exposure levels and the geographical distribution of vulnerable communities are, however, more complicated and less universal than often implied (Fecht et al., 2015). Relationships between socioeconomic and environmental risk factors have been revealed to diverge between study areas, status and scales of socioeconomic measurement, but population characteristics which explain these associations at a local level are still not fully understood (Goodman et al., 2011; Vrijheid et al., 2012).

Policy measures to control transport sector pollution is challenging to implement since transport emissions result from non-point sources where there is an absence of proof for individual responsibility (Abou-Ali and Thomas, 2011). Thus, alternative demand-side policy measures (e.g. controlling fuel prices through subsidy removal) can discourage owners from using their cars frequently and instead encourage them to seek alternatives, resulting in reduced congestion and pollution levels (Parry and Timilsina, 2015; Abou-Ali and Thomas, 2011). It has been proven that a 50% increase in fuel prices could lower congestion costs by US$22 million in the short-term and by US$69 million in the medium-term (TWB, 2018). Another study showed that imposing gasoline tax and removing fuel subsidies would reduce gasoline use by 43%, resulting in a 25% reduction in auto and microbus miles driven (Abou-Ali and Thomas, 2011). However, other studies showed that petrol price changes had no impact on air pollution (Barnett and Knibbs, 2014; Chen and Lin, 2015). Therefore, elucidating the effect of fuel price as an air pollution mitigation measure is still an open scientific question that has been investigated here.

Several studies have attempted to quantify the health impact and economic losses attributed to ambient $PM_{2.5}$ exposure levels that exceed health standards (Fantke et al., 2019; Kumar et al., 2020a; Maji et al., 2018; Nansai et al., 2020; Gustafsson et al., 2018). The health burden resulting from $PM_{2.5}$ exposure is quantified using exposure–response functions based on four components: the exposed population size; the baseline incidence rate; the effect estimated from epidemiological studies; and the change in air quality (Fann et al., 2012; Gustafsson et al., 2018).

Translating pollutant concentrations and exposure into the number of deaths caused and national economic losses occurred highlights this important issue for policy makers in more relatable terms. Literature has focused on estimating the health burden and economic losses caused by exposure to ambient $PM_{2.5}$ levels in several global cities. However, studies have not focused on the direct burden and losses incurred by anthropogenic activities such as working in certain industries or traffic commutes. Such assessments for short-term exposure, especially for in-car exposure, are rare and hence is one of the focus areas for this work.

As shown in Table 1, limited studies have reported PM exposure in transport microenvironments in cities in least developed, low-income or developing countries. A summary of relevant previous research reveals a lack of studies quantifying and comparing the length of hotspots on typical routes and variations in time spent at them in different cities (Table 1). Most cities follow the international trend where private cars remain a preferred means of transport; however, their focus has generally not been on estimating the potential inhaled doses of $PM_{2.5}$ at hotspots and the effect of fuel pricing on air pollution exposure in each city.

Studies have also not focused on health burden and economic cost evaluation of PM exposure in transport microenvironments. Our earlier work (Kumar et al., 2021) produced an internationally comparable in-car $PM_{2.5}$ exposure data across ten global cities (Section 2.1). Thus, this work aims to carry out an in-depth complimentary analysis for understanding the $PM_{2.5}$ hotspot lengths and time spent on the routes as a function of total commuting length/time in these cities and their association with potential inhaled doses, health burden (i.e. premature deaths) and socioeconomic (i.e. GDP, fuel pricing, economic losses) factors, and discussing the associated underlying reasons.

2. Methodology

2.1. Study area and data

Fig. S1 shows the location of the 10 cities studied across four regions: Asia (India, Bangladesh, China), Latin America (Colombia and Brazil), Africa (Tanzania, Malawi, and Ethiopia), and the Middle-East (Egypt and Iraq). The cities among them included: Dhaka (Bangladesh), Chennai (India), Guangzhou (China), Medellín (Colombia), São Paulo (Brazil), Cairo (Egypt), Sulaymaniyah (Iraq), Addis Ababa (Ethiopia), Blantyre (Malawi), and Dar-es-Salaam (Tanzania). A brief description of each city is as follows, and a summary of detailed information on cities' climatic and topographical features can be found in the Supplementary Information (SI) Table S1.

- **Dhaka** (DAC; 23.7N, 90.4E) is a densely populated megacity and the capital of Bangladesh. It is situated in southeast Asia and covers a total area of 1640 km^2. In 2018, the city's population accounted for 19.6 M (UN, 2018) with about 335 k cars (BRTA, 2018). The average elevation of DAC above the mean sea level (MSL) is ~5 m. DAC experiences four major seasons: winter (December-February), summer (March-May), monsoon (June–August), and post-monsoon (September-November). The climate in DAC is mostly tropical, with temperature ranges of 15–33 °C and relative humidity ranging from 37% in February to 74% in August, wind velocity varying from

Table 1
Summary of relevant studies on air pollution exposure assessment in transport microenvironments of least developed/developing countries.

City (Country)	Study focus	Key findings	Author (year)
Ten cities (Asia, Latin America, Africa and Middle-East)	Global assessment of PM exposure in cars across ten cities.	● Coarse particles dominated the PM fraction during windows-open while fine particles dominated during fan-on and recirculation. ● For windows-open, pollution hotspots made up to a third of the total route-length. ● For windows-open, $PM_{2.5}$ exposure during off-peak hours was 91% and 40% less than morning and evening peak hours, respectively.	Kumar et al. (2021)
Dhaka (Bangladesh)	$PM_{2.5}$ in different transportation modes.	● $PM_{2.5}$ in motorised areas was ~4-times and 2-times higher than the WHO standard and national standards, respectively, than in vehicle-free areas. ● Improving public transport services may reduce air pollution in Dhaka.	Hossain et al. (2019)
Chennai (India)	Effect of ambient CO levels on its in-car concentrations.	● Ambient concentration of CO at ~1 km away from a traffic intersection was ~74% lower than at the intersection. ● Hourly exposure of in-car CO during AC-On fresh air mode was ~1.5-times higher than AC-On recirculation and ~1.5-times less than windows-open.	Giri et al. (2020)
	Effect of modes of transport on $PM_{2.5}$ and $NO_{.2}$ exposure.	● Maximum exposure concentrations of $PM_{2.5}$ and NO_2 in the bus were 709 μg m^{-3} and 312 μg m^{-3}, respectively.	Raj and Karthikeyan (2019)
Vellore (India)	Commuter exposure concentrations and inhalation doses in traffic and residential areas	● Morning trips were significantly more polluted than afternoon trips in the traffic route, while in the residential route, afternoon trips had a slightly higher concentration. ● In traffic and residential roads, pedestrians and cyclists recorded maximum inhaled doses per trip, respectively, compared to other motorised transport modes.	Manojkumar et al. (2021)
Bangalore (India)	Use of personal samplers to measure exposure for assessing environmental justice	● Several methodological problems in calculating real exposures to commuters on an individual basis are addressed in the study. ● The findings do not support the environmental justice hypothesis for commuting in Bangalore, mostly because the gains of lower pollutant concentrations are compensated by higher-income groups' longer commute times.	Sabapathy et al. (2015)
Delhi (India)	Analysis of various transport modes to evaluate personal exposure to $PM_{2.5}$	● Closed AC transport modes were found to be the safest to avoid elevated $PM_{2.5}$ concentrations, but other conditions (such as time of day, car window open or closed) had a major impact on exposure levels. ● Walking, rickshaw, and non-AC vehicle transportation modes showed the highest average respiratory deposition doses among transport modes.	Maji et al. (2021)
Guangzhou (China)	Health risk of volatile organic compounds (VOC) in commuting modes.	● Exposure time is the most influential parameter for carcinogenic and non-carcinogenic risk, followed by ambient levels of VOCs and exposure duration. ● Subway, non-AC bus and bicycle are recommended for city dwellers to reduce health risks from traffic emissions.	Tong et al. (2019)
	Pollution exposure at bus commuter stations.	● Pollutant concentrations were significantly higher at bus stops compared with those at the fixed monitoring station (located away from the bus stop). ● Exposure of bus passengers to PM, NO_X and CO was higher than near roadside or at the bus stop.	Xu et al. (2016)
Zhengzhou (China)	Commute-related exposures to a variety of pollutants	● The travel mode usually described the greatest variability in pollutant exposure, in comparison to route, time of day, and background pollutant concentrations. ● Cycling emerged as the commuting mode with the maximum inhaled dose when breathing rate was taken into account to compute pollutant doses.	deSouza et al. (2021)
Nanjing (China)	Commuter exposure to particulate matters in four common transportation modes	● The majority of particles in a subway cabin come from the subway station, and the majority of particles in a bus cabin come from the ambient air, with little contribution from indoor sources. ● The amount of PM inhaled during a subway ride is lowest, while the amount inhaled while walking and cycling is>5 times higher.	(Shen and Gao, 2019)
Bogotá (Colombia)	Exposure to PM in transport microenvironments.	● Exposure to PM concentrations inside the fleet of diesel buses was significantly higher than exposure of pedestrians and cyclists. ● High pollution levels inside bus cabins can affect a large population.	Morales et al. (2017)
	Exposure to $PM_{2.5}$, black carbon (BC), and particle number in transport microenvironments.	● Commuter's exposure in public transport was ~3-times higher than for pedestrians. ● Exposure concentration to PM for commuters in a car was significantly lower than for commuters in other motorised transport modes.	Betancourt et al. (2017)
Bogotá (Colombia)	Personal exposure to air pollutants in a Bus Rapid Transit System	● Commuters in newer vehicles have slightly lower intake and inhaled doses of PM2.5, BC, and CO, suggesting that fleet renewal may have a disproportionately high effect on reducing population exposure to air pollutants ● The data in this study indicates that in-bus and in-station levels are many times higher than outdoor concentrations, independent of month-to-month variations in air pollution levels in the region.	Betancourt et al. (2019)
Bogotá and Medellín (Colombia)	Personal Exposure to $PM_{2.5}$ in the Massive Transport System	● Medellín Transport system(electric and gas natural vehicles) users are exposed to 5-times lower $PM_{2.5}$ levels than Bogotá Transport system (powered by diesel) users. ● The personal exposure in old and new vehicles in Bogotá was also found to be comparable due to the low proportion of new vehicles during the study period.	Castillo-Camacho et al. (2020)
São Paulo (Brazil)			

(*continued on next page*)

Table 1 (*continued*)

City (Country)	Study focus	Key findings	Author (year)
	Evaluating air pollutants from urban buses under real-world conditions.	● Incorporating buses with new technologies (electric buses) can have a significant impact of up to 40% on reducing NO and CO_2 emissions. ● Trace elements showed that vehicle emissions made substantial contributions to fine and coarse fractions of hazardous metals, such as Cr, Zn, V, and Pb.	Nogueira et al. (2019)
Londrina (Brazil)	Commuter exposure to BC on diesel buses, bicycles and walking	● BC concentrations for the two active modes were lower than those inside buses, with bus/walk and bus/bicycle ratios of up to six. ● High in-bus concentrations were found on congested roads due to increased traffic density surrounding the bus, lower driving speed and frequent stops.	Targino et al. (2018)
	Variations in individuals' exposure to BC particles during their daily activities	● There were no statistical differences in total average exposure and dose by gender. ● Exposure was higher on bus journeys, while with pedestrians, cyclists and bus drivers affected by lower exposure.	Carvalho et al. (2018)
Curitiba (Brazil)	Bus commuter exposure and the impact of switching from diesel to biodiesel	● Switching from diesel to biodiesel could help minimise commuters' exposure to BC particles on Bus Rapid Transit buses, but it would need to be complemented with after-treatment technologies to reduce emissions. ● Further exposure reductions (especially to peaks) could be accomplished by switching bus routes to avoid passing through narrow urban street canyons.	Targino et al. (2020)
Cairo (Egypt)	Car users exposure to PM pollution	● $PM_{2.5}$ was highest during windows-open car settings. ● PM concentrations were higher during evening peak hours than morning peak.	Abbass et al. (2020)
Sulaymaniyah (Iraq)	Characterisation and biological effects of PM_{10}	● A passive sampler was used to collect dust particles at three different sites. ● Dust from industrial and urban sites triggered cytotoxic and genotoxic effects, whereas minor effects were observed for rural sites.	Arif et al. (2018)
Addis Ababa (Ethiopia)	Commuter exposure to PM and total VOCs	● Highest and lowest values for PM (diameter ≤ 7 and ≤ 10 μm μm and total suspended particles) were noticed at Addis Ketema and Gulelle sub-cities. ● Highest and lowest values for total VOCs were found at Addis Ketema and Nefas Silk-Lafto sub-cities.	Embiale et al. (2019)
Blantyre (Malawi)	Air quality assessment of CO, NO_2 and SO_2 levels	● Variations in hourly, diurnal, monthly and seasonal CO, SO_2 and NO_2 indicated the considerable contribution of industrial and transportation activities in the city. ● CO levels (2.5 mg m^{-3}) were below the Malawian limit value (10.3 mg m^{-3}) while NO_2 (4.0 mg m^{-3}) and SO_2 (8.6 mg m^{-3}) were significantly higher.	Mapoma et al. (2014)
Dar-es-Salaam (Tanzania)	Risk evaluation of roadside levels of gaseous pollutants and PM	● Hourly average NO_2 concentration ranged from 18 to 53 μg m^{-3}. The maximum hourly NO_2 concentration at 53 μg m^{-3} was below the WHO guideline. ● Risk assessment focused on people who spend a significant time near roads.	Jackson (2005)

7.5 to 18.4 km/h, and with wind direction is mostly from either north or south.

- **Chennai** (CHE; 13.0N, 80.2E) is the capital city of the south Indian state of Tamil Nadu. CHE covers a total area of 426 km^2 and its metropolitan area covers 1189 km^2. In 2018, it had a population of over 10.4 M (UN, 2018) with about 1 M cars in 2016 (SYBI, 2017). The average elevation of CHE above the MSL is ~15.8 m. CHE experiences four major seasons: winter (December-February), summer (March-May), monsoon (June-August), and post-monsoon (September-November). The weather is generally hot and humid, with January being the coldest month with the daily minimum temperatures of 21 ± 2 °C, and May the hottest month in the year with the daily maximum temperatures at 36 °C. The average annual relative humidity is 70%. The region is considered a rain shallow region as during the pre-monsoon period it receives only about 32% rainfall. The dominant wind direction, observed from Chennai airport, is towards the south (21%), followed by the west (16%) and the east (15%) (Kumar et al., 2020a).
- **Guangzhou** (CAN; 23.1N, 113.2E) is a city in south-eastern China, located in the heart of the Pearl River Delta. CAN covers a total area of 7434 km^2. In 2018, it had a population of over 14.9 M (GBS, 2019) and a car fleet of around 1.8 M in 2018 (GPB, 2019). The average elevation of CAN above the MSL is ~21 m. CAN experiences four major seasons: winter (December-February), spring (March-May), summer (June-August), and autumn (September-November). CAN climate is humid subtropical. The average annual precipitation, humidity and temperature variation are 1690 mm, 68–78%, and 18-22℃, respectively (Rahman et al. 2019).
- **Medellín** (MDE; 6.2N, 75.5W) is the second-largest city in Colombia. MDE covers an area of 1165 km^2. In 2018, it had a population of around 4 M (UN, 2018), and a car fleet of over 467 k in 2018 (AMVA, 2012). The average elevation of MDE above the MSL is ~1495 m. MDE has a tropical climate with an annual mean temperature of 21.5 °C and relative humidity of 67%. The precipitation is at its maximum during March-May and October-November, with an annual average of 1687 mm.
- **São Paulo** (SAO; 23.5S, 46.6W) is the most economically important region of Brazil. SAO covers a total area of 1521 km^2. In 2018, it had a population of around 21 M (UN, 2018) and a car fleet of over 5 M in 2017 (CETESB, 2019). The average elevation of SAO above the MSL is ~769 m. The region is characterised by a dry season with comfortable temperatures (winter, June to August), a rainy season in which it is hot and wet (summer, December to March), and intermediate conditions (in spring and autumn) with an annual precipitation average of 1340 mm. SAO has a humid subtropical climate, with minimum daily temperatures in July of 18.5 °C and minimum relative humidity in August of 78.7%.
- **Cairo** (CAI; 30.0N, 31.2E) is the capital of Egypt and is a densely populated megacity. CAI covers a total area of 3085 km^2. In 2018, it had a population above 20 M (UN, 2018) and its car fleet was around 2.4 M in 2017 (CAPMAS, 2017). The average elevation of CAI above the MSL is ~23 m, with annual precipitation between 22 and 29 mm

and temperatures between 18 and 45 °C (Hassanien and Abdel-Latif 2008). CAI has a typically hot desert climate.

- **Sulaymaniyah** (SUL; 35.5N, 45.4E) is one of the largest cities of the Kurdistan Region in Iraq. In 2018, it had a population of about 1.9 M (CPP, 2019) with a car fleet of around 80 k (KRSO, 2019). The average elevation of SUL above the MSL is ~882 m. SUL experiences four main seasons: winter (December-February); spring (March-May); summer (June-August); and autumn (September-November). SUL has a semi-arid climate with an annual average temperature of 18.5 °C and relative humidity ranging from 70.3% to 24.9. The annual precipitation is around 600 mm and a dry season (summer) with no rain. The wind comes from the southwest direction at an annual average of 2.1 m/s.
- **Addis Ababa** (ADD; 9.0N, 38.7E) is the capital of Ethiopia. It covers a total area of 527 km^2. In 2018, it had a population of over 4.4 M (UN, 2018), and its car fleet was 750 k (EMT, 2019). The average elevation of ADD above the MSL is ~2355 m. ADD experiences four main seasons: winter (December-February), spring (March-May), summer (June-August) and autumn (September-November). ADD has a subtropical highland climate. The temperature ranges from a minimum of 8 °C to a maximum of 25 °C. The rainfall ranges from a minimum of 7 mm (November/December) to 280/290 mm (July/August). The relative humidity ranges from 45.5% in December to 79.5% in July.
- **Blantyre** (BLZ; 15.7S, 35.0E) is the main commercial center of Malawi and its second largest city. It covers a total area of 240 km^2. In 2018, it had a population of around 0.8 M (CPP, 2019) and a car fleet of about 130 k in 2015 (CEIC, 2016). It has diverse topography and an average elevation above the MSL ranging from 780 to 1612 m. It has a hot rainy season (mid-November to April) and relatively cold and dry season in austral winter (mid-May to mid-August). The district is hilly and mountainous and has a sub-tropical climate. The average of temperature ranges from 19 °C during the cold to 26 °C during the hot seasons (Mapoma et al., 2016). The mean annual rainfall is 1,122 mm and about 80% falls between November and March.
- **Dar-es-Salaam** (DAR; 6.8S, 39.2E) is the capital of Tanzania. It covers a total area of 1590 km^2. In 2018, it had a population of around 6 M (UN, 2018) and its car fleet was around 707 k in 2012 (Kiunsi, 2013). The average elevation of DAR above the MSL is ~24 m. DAR has a tropical wet and dry/savanna climate. DAR experiences two rainy seasons: the short rainy season (October to December); and the long rainy season (March to May), with maximum and minimum temperatures of 35 °C and 25 °C, respectively. DAR has an annual rainfall of approximately 1,200 mm and an annual relative humidity of 77.9%.

In order to carry out a detailed analysis of hotspots, socioeconomic correlations, the impact of fuel pricing on pollution exposure levels, national health burdens and economic costs, we used a primary set of $PM_{2.5}$ data collected simultaneously from the ten global cities in 2019. These $PM_{2.5}$ data were collected every one-minute using a portable laser particle counter from the backseat of a passenger car. The same route and the same car in each city were used for all runs including three car settings (windows-open; windows-closed with fan-on; windows-closed with recirculation) and three times during the day: morning peak (MP); evening peak (EP); off-peak (OP). Owing to much adverse health impacts compared with its larger-sized counterparts, we focused on $PM_{2.5}$ exposure data during windows-open settings as the highest concentrations were recorded compared with windows-closed (fan-on and recirculation). Moreover, the inside to outside concentration ratio of $PM_{2.5}$ are usually reported to be close to unity during windows-open condition (Matthaios et al., 2020; Kumar et al., 2021), substantiating the fact that the windows-open scenario can be considered as a proxy for on-road ambient concentrations. SI Table S2 presents the summary of statistics on the average route length and the corresponding time taken to complete the trips under windows-open setting. Further description on the data collection, type of passenger car (SI Table S3) and the route characteristics can be found in SI Sections S1 and S2, respectively. To ensure the quality control and harmonisation of the data, we carried out co-location measurements over five days where all the aerosol equipment (Dylos OPCs) were co-located with a research-grade optical particle spectrometer (GRIMM model 11-C) to assess the inter-comparison among the Dylos OPCs as well as their comparison with research-grade equipment. High agreement was found among all monitors as the Pearson correlation coefficient (r) ranged from 0.92 to 0.99 $PM_{2.5}$ (SI Fig. S2). A reasonable good correlation was found between the monitors and the research-grade equipment (GRIMM), with r ranging from 0.82 to 0.91 for $PM_{2.5}$ (SI Fig. S3). Further details on data collection, route selection, and quality assurance can be found in Kumar et al. (2021).

2.2. Hotspot analysis

Hotspots along the routes in cities studied were identified by counting data points exceeding 90th percentiles (P90) of the one-minute average $PM_{2.5}$ concentrations during windows-open setting. The P90 was calculated for each city using the overall dataset, including the three measured car settings, following the methodology described in Kumar et al. (2021). To carry out the hotspot analysis, $PM_{2.5}$ concentrations were used to compare the inhaled doses at the hotspots versus those at free-flow segments of roads across the ten cities (Section 2.3). Furthermore, the inhaled doses at hotspots were compared to different socio-economic parameters for each city including: gross domestic product; the value of statistical life; and road density (Section 2.3). To investigate the effect of fuel price variations on $PM_{2.5}$ concentrations, relevant data was sourced for each city from secondary sources including: fuel prices; city specific congestion parameters such as car density and average speeds; population size; number of cars per inhabitant (Section 2.4); and the inhaled doses per unit distance (Section 2.3). Finally, health burden and economic losses were derived using published methodologies (Section 2.5) utilising $PM_{2.5}$ concentration data, baseline mortality rates, car commuter population size and value of statistical life. Data processing and statistical analyses for this section were carried out using Excel and R statistical software (R Core Team, 2019) with the software package *openair* (Carslaw and Ropkins, 2012).

2.3. Inhaled dose estimation

The data collected under windows-open setting was used to quantify the time spent in hotspots or free-flow conditions and their potential inhaled $PM_{2.5}$ doses. For each city, the average time spent in hotspots was calculated as the number of $PM_{2.5}$ data points (one-minute averaged) exceeding P90 (Section 2.2); the rest of the data points were considered as occurring during free-flow conditions. It is worth noting that because the P90 was calculated using the data collected in all three car settings (as described in SI Section S1), therefore the time spent in hotspots during windows-open setting is not always 10%. The mean lengths of hotspots (Table 5) were calculated by multiplying the average speed of the car during the journey (Table 2) and average time spent in hotspots (Table 5). The quantity of potential inhaled dose is a function of the $PM_{2.5}$ concentration (C; μg m^{-3}) inside a car, time spent during a journey and the respiratory rate of the commuter, which is influenced by gender, age and health. We estimated inhaled dose both by per unit time basis (ID_t; μg $kg^{-1}h^{-1}$) and per unit distance travelled basis (ID_d; μg km^{-1}). ID_t during a car journey was estimated using Eq. (1) (USEPA, 1992):

$$ID_t = (C \times IR)/BW \quad (1)$$

where IR (m^3 h^{-1}) is the inhalation rate, which was taken as 0.8184 m^3 h^{-1} for adult males while seated (Hinds, 1999), and BW (kg) is bodyweight for an individual, which was taken as an average of 75.4 kg for

the age group of 30–44 years (Nogueira et al., 2020). Since the estimated inhaled doses for male (0.8184 $m^3\ h^{-1}$) and female (0.6642 $m^3\ h^{-1}$) follow the same trend due to the constant value of IR used in Eq. (1), the discussion remains valid for both the genders. Therefore, we only refer to male doses in the subsequent discussion for the purpose of brevity. The ID_d allowed the elimination of the differences in route length and the time spent inside cars among the ten cities, thus allowing a relative comparison to be made, as shown by Eq. (2):

$$ID_d = (C \times IR \times t)/l \quad (2)$$

where t (h^{-1}) is the time of each trip and l (m) is the distance travelled along the route in each city. Eqs. (1) and (2) also allowed us to calculate the percentage of time spent at hotspots, percentage of inhaled $PM_{2.5}$ doses, and the ratio of $PM_{2.5}$ levels at hotspots and free-flow conditions.

Further analysis enabled us to assess the relationships between socioeconomic factors of cities and their hotspot parameters. We considered the following socioeconomic factors in our analysis: city-specific gross domestic product per capita (GDP; US$), value of statistical life (VSL; US$/person), road density, fuel prices, health burden and economic losses. City-specific GDP per capita is shown in SI Table S4. VSL is an economic value that is used to quantify the benefit of avoiding a fatality and differs from one country to another (Table 3), and road density (D_R; km^{-1}) which is a ratio of the total length (L; km) of all roads in the administrative area of the city (A; km^2) to the total population (P) of the city (Eq. (3)):

$$D_R = L/(A \times P) \quad (3)$$

The details of the administrative area of cities, the total population living in the respective administrative area, and length of different categories of roads in the cities are provided in SI Table S4.

2.4. Fuel pricing and $PM_{2.5}$ concentrations

Parameters used for this analysis include fuel prices, average $PM_{2.5}$ concentrations, inhaled doses per unit distance, city-specific time spent in traffic per year such as car density and average speeds, population size and the number of cars per inhabitant (Table 2). Fuel prices (US$ per litre) can be considered as a reflection of subsidy levels in a country. For instance, lower fuel prices indicate higher subsidies considering a uniform international market price for the fuel. Average in-car $PM_{2.5}$ concentrations during windows-open and the corresponding total daily inhaled doses indicate levels of air pollution that car commuters are exposed to during travel. We considered the average speed as a measure of congestion since higher speeds mean a relatively higher free-flow of traffic and vice-versa. Finally, the number of cars per inhabitant is considered an indication of both the purchasing power in a country as well as commuter reliance on cars due to a lack of transport alternatives. The results of this analysis were used to draw correlations between fuel pricing and air pollution levels (Section 3.3).

2.5. Health burden and economic cost of $PM_{2.5}$ exposure

We estimated the health burden resulting from exposure to $PM_{2.5}$ levels during car commutes to the exposed population of car commuters (CC). *CC* (# of car commuters) in each city is estimated as a product of car density (# of cars/city) and average car occupancy (# of car commuters/car), using the Eq. (4) and the parameters listed in Tables 2 and 3 show the exposed population (CC) and % of CC from city population

$$CC = Car\ density \times Average\ car\ occupancy \quad (4)$$

HB was estimated using Eq. (5) (Maji et al. 2018; Kumar et al., 2020a; Li et al. 2019; Nansai et al. 2020).

$$HB = [(RR - 1)/RR] \times B \times CC \quad (5)$$

where *HB* (# of premature deaths) is the health burden; *B* (deaths per 100,000 people) is the baseline mortality rate within the population of interest; and *CC* (# of car commuters) is the exposed population of car commuters (Eq. (4)). *RR* (-) is the relative risk of mortality when an entire population is exposed to pollution levels that exceed a reference concentration (Maji et al. 2018; Nansai et al., 2020). Numerous types of RR functions have been developed and used in the literature (e.g. Fantke et al., 2019; Hu et al., 2015; Maji et al., 2018; Orellano et al., 2020; Shang et al., 2013). For example, some studies have assumed a linear relation between mortality and $PM_{2.5}$ exposure; however, these tend to underestimate the number of premature deaths (Li et al., 2019). Integrated exposure response (IER) functions have been adopted by several studies that focused on indoor microenvironments such as vehicles (Xiang et al. 2019; WHO 2016); however, there is considerable uncertainty about the IER function and its fitted parameters. Statistical time-series analysis carried out in epidemiology studies have been typically used for short-term exposures where log-linear functions have been employed for both long-term (one-year or more) and short-term (defined as a few hours to one day) exposures (Maciejewska, 2020; Orellano et al., 2020; U.S. EPA, 2010; WHO, 2006; Zheng et al., 2021). Considering the above limitations and the context of our work involving short-term exposure, we adopted the log-linear function (Azimi and Stephens, 2020; Ji and Zhao, 2015). RR is estimated using Eq. (6) that has been used in a diverse range of previous studies (e.g. Azimi and Stephens, 2020; Kumar et al., 2020a; Shen et al., 2020; Maji et al., 2018; U.S. EPA, 2010). *RR* is estimated using Eq. (6) (Kumar et al., 2020a; Maji et al., 2018).

$$RR = exp(\beta_{PM2.5}(C_i - C_0)) or C_i > C_0 \quad (6)$$

$$RR = 1 \quad \text{for } C_i \le C_0$$

where C_i is the average in-car $PM_{2.5}$ concentration under windows-open setting, as listed in Table 2 for each city; C_0 is the threshold concentration below which no additional health impacts are calculated (Maji et al. 2018). The average exposure concentrations are based on measurements taken on a specific route in each city that is considered a representation of a car commuter's average exposure levels despite the variations such representation might introduce (Abbass et al., 2021). Standard deviation ranges of C_i are taken into consideration for producing *HB* numbers with 95% confidence intervals (CI) as listed in Table S5. For the purpose of comparison, average in-car $PM_{2.5}$ concentrations under recirculation setting (Table S5) are also used to produce estimates for *HB* (Section 3.4). WHO guidelines suggest annual mean $PM_{2.5}$ concentration at 10 μg m^{-3} and 24-hour mean at 25 μg m^{-3} (WHO, 2018). Here, we set C_0 to be equal to the daily mean exposure standards of 25 μg m^{-3}, which was also used as a threshold in a study that investigates the impact of daily excess $PM_{2.5}$ concentrations hours on mortalities (Lin et al., 2017). $\beta_{PM2.5}$ is the exposure–response coefficient, indicating an increase in mortality due to an increase in $PM_{2.5}$ concentrations; it is taken as 0.038% per 1 μg m^{-3} increase in $PM_{2.5}$, based on a systematic review of studies on short-term (24-hr averages) exposure to air pollution and daily mortality of all ages (Hu et al., 2015; Kumar et al., 2020a; Shen et al., 2020). Most studies that estimate mortality associated with $PM_{2.5}$ exposure focus on long-term ambient exposures despite the evident impact of short-term $PM_{2.5}$ exposure on all cause mortalities and morbidities (e.g. Maciejewska, 2020; Orellano et al., 2020; Li et al., 2019). There is limited work that investigates mortalities caused by short-term exposures based on 24-hr average $PM_{2.5}$ concentrations (e.g. Maciejewska, 2020; Orellano et al., 2020; Li et al., 2019; Akbarzadeh et al., 2018; Kloog et al., 2013) while most recent works have extrapolated hourly concentrations during commuting to 24-hr average PM concentrations (e.g. Zheng et al., 2021). These studies assessed the correlation between $PM_{2.5}$ exposure concentrations preceding the incident of mortality by one or two days (Guiqin et al., 2020; Maciejewska 2020; Kloog et al., 2013; U.S. EPA, 2010). This current work adopts these basic concepts and extends to

provide a unique insight by translating the cumulative impact of daily short-term exposure during car commutes over one year into the expected premature deaths (Abbass et al., 2021).

B in Eq. (5) is country-specific all-cause mortality rates per 100,000 people (Table 3; GBD, 2019). It is reasonably assumed that *B* for each city is equal to the country-specific mortality rate (Bjorn, 2019) due to the lack of availability of city-specific data for all cities. Moreover, it was preferable to reference our data to a common source (GBD, 2019) to reduce uncertainties and make estimates comparable. This figure is used to derive the hourly baseline mortality by dividing the annual rate into 365 days and 24 h, to accommodate for the hourly exposures focused on in this work (Abbass et al., 2021).

Since *RR* and *B* are based on hourly observations and rates, the *HB* indicates deaths resulting from hourly exposure to excess $PM_{2.5}$ concentrations during car commutes at peak and off-peak hours. Average concentrations (C_i) during MP, OP and EP are used to produce an RR corresponding to each time of the day. The whole exposed population of car commuters (CC) are used with each of the *RR*'s derived for the three periods (MP, OP and EP) as it is assumed that the whole car commuting population will probably travel for at least an hour during all three-time segments throughout the year. Time spent in traffic by a car commuter for each city is derived using field data collected from the campaign and normalised over the average trip length across all cities (Table S5). It is assumed that a typical commuter does three trips (MP, EP, OP) per day during weekdays (5 days/week) giving the total number of hours spent in traffic per year for this study (Table 3). The percentage of time spent in traffic in each time segment (MP, OP and EP) is derived for each city based on the field campaign data (Table S5). Then annual *HB* is calculated for each time of the day and summed to produce the total (and per 100,000 exposed population of car commuters) *HB* attributed to the excess $PM_{2.5}$ car exposure.

The $\beta_{PM2.5}$ used to calculate *RR* is based on 24-hr average while the

Table 2
The summary of the city-specific data utilised for fuel price versus $PM_{2.5}$ pollution exposure analysis; and number of car commuters in each city estimated using Eq. (4), city population and the percentage of car commuters for each city.

Cities	Fuel price (US$ L^{-1})[a]	Average $PM_{2.5}$ concentrations (μg m^{-3})[b]	Total daily inhaled dose (μg km^{-1})[c]	Average speed (km hr^{-1})[d]	Car density (cars/city)	Population size (#) for 2018[o]	Number of cars/ inhabitants[r] (#)	Exposed Population (car commuters exposed to pollution)	% of car commuters from city population
DAC	1.05	62	3.7	14	335,660[e]	19,578,000	0.02	503,490	2.6
CHE	1.14	65	2.4	23	1,043,500[f]	10,456,000	0.10	1,200,025	11.5
CAN	0.94	72	1.4	43	1,869,270[g]	1,4900,000[p]	0.13	3,177,759	21.3
MDE	0.56	23	1.2	15	466,974[n]	3,934,000	0.12	1,046,021	26.6
SAO	0.76	26	1.3	15	5,249,040[i]	21,650,000	0.24	8,083,521	37.3
CAI	0.54	61	2.0	24	2,429,797[j]	20,076,000	0.12	3,012,948	15.0
SUL	0.63	22	0.6	34	80,264[k]	1,879,000[q]	0.04	176,580	9.4
ADD	0.59	75	3.6	18	750,000[l]	4,400,000	0.17	2,775,000	63.1
BLZ	0.92	83	3.1	20	129,996[m]	800,264[q]	0.16	194,994	24.4
DAR	0.73	82	7.3	9	707,521[n]	6,048,000	0.12	2,617,827	43.3

[a] GPP (2020). Average fuel prices were taken between June and August 2020.

[b] Average $PM_{2.5}$ concentrations for windows-open runs for each city.

[c] Inhaled dose is calculated using Eq. (5) in Kumar et al. (2021) and averaged for windows-open trips.

[d] Average car speed during trips for each city.

[e] BRTA (2018) for whole city.

[f] SYBI (2017).

[g] GPB (2019), for whole city.

[h] SIGAIRE (2017), for whole city.

[i] CETESB (2019), for the Metropolitan Area of São Paulo.

[j] CAPMAS (2017), for Greater Cairo which is the megacity made up of Cairo and Giza.

[k] KRSO (2019), for whole city.

[l] EMT (2019), for whole city;

[m] CEIC (2016), for whole city (most reference was not available).

[n] Kiunsi (2013), for whole city.

[o] UN (2018).

[p] GBS (2019).

[q] CPP (2019).

[r] The number of cars per inhabitant is calculated by dividing car density (number of cars in each city) by its population (number of inhabitants).

concentrations are based on hourly average observations. We assume that the temporal variations in the exposure–response coefficient used to calculate *RR* provide preliminary estimates on the mortalities caused by in-car exposure to $PM_{2.5}$ concentrations since the data on the impact of certain hours in the day (car commutes in this case) on mortality rates are unavailable, especially for the studied cities. Also, $\beta_{PM2.5}$ indicates a percentage increase in mortalities for every corresponding 1 μgm^{-3} increase in $PM_{2.5}$ concentrations, regardless of exposure time. However, the calculations need to be modified to reflect the fraction of time spent in this microenvironment (Azimi and Stephens, 2020). Ideally 24-hr average $PM_{2.5}$ concentrations should be used to be consistent with the exposure–response coefficient adopted from literature. However, varied approaches are applied. For example, Zheng et al. (2021) used PM exposure during other activities throughout the day, in addition to commuting, such as sleep and work to derive the average daily $PM_{2.5}$ concentrations to be able to use daily *RR* values. However, this approach has not been adopted in this study due to unavailability of data on other daily activities in the ten cities but also because the aim of this work has been to focus on in-car exposure related health impacts.

Most epidemiological studies are focused on the exposure to ambient $PM_{2.5}$ concentrations despite the fact that $PM_{2.5}$ exposure in microenvironments like households, schools and vehicles, can account for a substantial proportion of ambient $PM_{2.5}$ exposure-related total mortalities such as 40–60% in the United States (Azimi and Stephens, 2020), 71–87% in urban China (Xiang et al., 2019) and 81–89% on a global scale (Ji and Zhao, 2015). Nevertheless, exposure–response functions derived for ambient $PM_{2.5}$ exposure can be used for exposure in a microenvironment setting, provided that coefficients are rescaled for population size (Milner et al., 2017). Furthermore, our study focuses on windows-open setting for in-car $PM_{2.5}$ exposure, which is a proxy for on-road ambient concentrations (Kumar et al., 2021; Matthaios et al., 2020). Hence, it was considered acceptable to use Eqs. (5) and (6) to derive health burden caused by in-car $PM_{2.5}$ exposure.

Economic loss (EL; US$) is quantified based on the probable number of premature deaths and the Value of Statistical Life (*VSL;* US$) (Kumar et al., 2020a; Viscusi and Masterman, 2017), using Eq. (7).

$$EL = HB \times VSL \tag{7}$$

3. Results and discussion

3.1. Inhaled doses at hotspots

Fig. 1 shows the density plot of in-car $PM_{2.5}$ concentrations measured under windows-open in all studied cities during MP, EP and OP hours. These plots show areas where values are more concentrated over a particular range of $PM_{2.5}$ concentrations and also indicate how differently the hotspots condition frequency occurs in each city. Similar behaviour regarding the $PM_{2.5}$ concentration distribution may be observed in some cities. For example, ADD, BLZ, and DAR show a low-density spread over the concentration range, especially during morning peak hours as opposed to those (MDE, SAO, and SUL) having stark peaks in a small concentration range. The hotspots frequency of $PM_{2.5}$ concentrations was consistently lower during OP hours for all the cities, indicated by their shapes being mostly more skewed to the left during OP hours than other times of the day. The exception was CAI, where the EP hours showed slightly lower occurrences of extreme values than OP (mid-day) hours (Fig. 1) mainly because mid-day is not considered OP

Table 3
The summary of key parameters used to calculate the health burden and economic losses using Eqs. (3)–(6). ΔC ($C_i - C_o$) is the difference between the reference (25 $\mu g\ m^{-3}$) and average observed concentrations for each city and time of the day. *RR* is estimated using ΔC and $\beta_{PM2.5}$ is calculated based on a 0.038% increase per 1 $\mu g\ m^{-3}$. When C_i do not exceed C_o, the value of ΔC is denoted by (-) and RR is 1.00, as indicated in Eq. (6).

Cities	ΔC ($\mu g\ m^{-3}$)			RR			Baseline mortality (B)[a] (deaths per 100,000 people) in 2019	Car occupancy (passengers/ car)	Time spent in traffic/ year (hours)	VSL ($ million)[k]
	MP	OP	EP	MP	OP	EP				
DAC	40	30	42	1.84	1.40	1.96	533.44	1.5[b]	1213	0.205
CHE	49	28	43	2.48	1.36	2.05	675.31	1.2[c]	600	0.275
CAN	83	26	31	13.97	1.28	1.45	749.00	1.7[d]	344	1.364
MDE	12	–	–	1.06	1.00	1.00	516.32	2.2[e]	782	1.228
SAO	14	–	–	1.08	1.00	1.00	651.32	1.5[f]	973	1.695
CAI	62	24	22	4.21	1.25	1.21	566.83	1.2[g]	643	0.575
SUL	7	–	–	1.02	1.00	1.00	426.44	2.2[g]	481	1.001
ADD	111	12	25	109.82	1.06	1.28	520.49	3.7[h]	850	0.102
BLZ	72	18	83	7.13	1.14	14.06	632.63	1.5[i]	665	0.058
DAR	81	31	57	12.03	1.45	3.50	624.56	3.7[j]	1638	0.158

[a] GBD (2019), All causes deaths per 100,000 both sexes, all ages.

[b] Labib et al. (2014).

[c] STO (2014).

[d] Cox (2019).

[e] AMVA (2012).

[f] Farmer (2020).

[g] Osra (2016).

[h] TMCRTE (2009).

[i] Fraser and Haworth (2017).

[j] Assumed Dar-es-Salam car occupancy is the same as Addis Ababa.

[k] Viscusi and Masterman (2017).

on the chosen route in Cairo, rather it has been reported as between midnight and sunrise (Nakat et al., 2013). The MP hours showed the highest frequency of hotspot conditions in all cities, except in CHE and DAC, where the frequency of extreme values during MP and EP hours were similar despite higher traffic congestion during evenings shown by longer trip durations compared to MP (Fig. S4). This might be due to favorable meteorological conditions (wind speed) during evening hours that contribute to the dispersion of pollutants. These results demonstrate that, in most cities, relatively high concentrations of $PM_{2.5}$ are more frequent during MP hours whilst low concentrations occur more frequently during OP hours.

The values of P90 during windows-open across cities varied from 34 μg m^{-3} (SUL) to 117 μg m^{-3} (DAR), Fig. 1. $PM_{2.5}$ concentrations in free-flow driving conditions greatly varied among the cities (Table 4). African and Asian cities (ADD, BLZ, DAR, DAC, CHE, and CAN) showed relatively higher concentration levels of $PM_{2.5}$ at hotspots compared with Latin American (SAO, MDE) and Middle Eastern cities (SUL). The increase in hotspot concentrations compared with those of free-flow conditions ranged from 2-times (CHE) to 3.5-times (CAN and SUL). This range is greater than that observed in a small town in the UK, where traffic intersections can result in 16% higher $PM_{2.5}$ compared with those on the rest of the route with free-flow conditions (Kumar and Goel, 2016).

In order to understand the magnitude of the impact of hotspots compared to free-flow conditions in the total potential inhaled dose, we calculated a statistical summary of $PM_{2.5}$ concentrations in all the cities studied, both during free-flow and hotspots driving conditions during windows-open car setting (Table 5). The time-based inhaled doses ranged from 0.59 (SAO) to 1.78 (BLZ) μg $kg^{-1}h^{-1}$ at the hotspots, whereas relatively lower values of 0.17 (SUL) to 0.71 (DAR) μg $kg^{-1}h^{-1}$ were recorded during free-flow (Table 5). The distance-based inhaled doses provided a better understanding of exposure resulting from the hotspots emerging from traffic congestion. These ranged from 0.4 to 5.9 μg km^{-1} and 1.5–14.3 μg km^{-1} for free-flow and hotspots, respectively. DAR recorded the highest inhaled doses (14.3 μg km^{-1}), followed by the other African cities (ADD and BLZ), and along with DAC displayed comparatively higher values of 6–8.1 μg km^{-1} (Table 5). The highest inhaled doses for DAR are due to higher $PM_{2.5}$ concentrations in free-flow conditions combined with longer time spent at hotspots (Table 5). Other factors such as presence of street canyons along the routes may have contributed to a disproportionate effect on concentration accumulation on some part of the routes but this information was not available precisely to be able to apportion their effects. Conversely, other cities (SAO, MDE, CAI, CHE and CAN) reported a lower range (2.3–3.7 μg km^{-1}; Table 5). The ratio of distance-based free-flow to hotspots inhaled doses ranged from 2 to 3.5, which followed the corresponding $PM_{2.5}$ concentration ratios (Table 4). Interestingly, cities (MDE, SUL and CAN) showing relatively lower inhaled doses at hotspots displayed the highest hotspot $PM_{2.5}$ doses/free-flow $PM_{2.5}$ doses of 3.4 to 3.5. These findings highlight that in these cities the identification of hotspot locations is important, and also that in other cities car commuters are exposed to high concentrations in both free-flow and hotspot conditions. The vehicle fleet is quite different among the studied cities, as shown in SI Table S6. Interestingly, the $PM_{2.5}$ concentration appears to increase with the number of buses per 10,000 inhabitants in cities (Fig. S5), indicating that although cities such as BLZ and ADD may need to consider cleaner buses. In contrast, a lower number of buses per inhabitant in cities like SAO and MDE associated with low $PM_{2.5}$ concentrations can be associated with a greater availability of underground trains, which use electricity. Finally, it was observed that the high number of two- and three-wheeler vehicles also seems to contribute to the high concentrations of $PM_{2.5}$ in CHE and DAC, while in MDE the contribution of these kinds of vehicles does not seem to be relevant to increased $PM_{2.5}$ concentration. In addition, driving routes varied from single to double road lanes. The on-road environment is usually turbulent due to the movement of the vehicles (e.g., Carpentieri et al., 2012) and the first few meters of the road is generally considered as a well-mixed environment (Kumar et al., 2009). However, the spatial concentration gradients could be expected, which are challenging to capture through in-car studies (e.g., Capentieri and Kumar, 2011). Both lanes were used during the monitoring, following the left- or right-hand driving rules in the studied cities. For example, CAN, MDE, SAO, CAI, SUL, and ADD used right-hand lanes of the road as opposed to the other cities using right-hand lanes (SI Table S6).

A more comprehensive understanding of $PM_{2.5}$ inhalation in hotspots and free-flow conditions emerged by plotting the percentage time spent in hotspot and free-flow driving conditions with the corresponding percentage of the inhaled $PM_{2.5}$ doses (Fig. 2b). The mean time spent in the car at hotspots across the cities accounted for only about 16% (SAO) to 28% (ADD) of the total time spent on each route but corresponded to much higher inhaled doses, 30% (CHE) to 56% (ADD) of the total commuting doses (Fig. 2b). Such a disproportionate distribution of inhaled doses has also been reported in previous work. For example, Goel and Kumar (2015) found that as little as 2% of the time spent at traffic intersections during a car commute corresponded to up to 25% of total respiratory deposition doses during a car trip. Cross-comparison of cities showed that more than half of the inhaled $PM_{2.5}$ doses along the route accounted for spending only 26% (CAN) and 28% (ADD) of total time at hotspots. SUL and MDE followed the trend by showing high hotspot to free-flow $PM_{2.5}$ doses by reporting 41% of inhaled $PM_{2.5}$ at hotspots, which corresponded to only about 17% of the total commuting time. The contribution of hotspots to the amount of inhaled $PM_{2.5}$ varied according to the time spent and the $PM_{2.5}$ concentrations at the hotspots. Irrespective of the cities, the time spent at hotspots was found to be disproportionately lower compared with the inhaled doses (Fig. 2b) suggesting that a relatively small time spent at hotspots could still lead to a significant portion of total inhaled doses during a car commute and the policies targeting the hotspot lengths could bring considerable health benefits to city dwellers.

3.2. Socioeconomic factors and hotspots parameters

The relationship between the hotspots-related parameters and socio-economic factors were assessed for each city to understand their mutual relationship and to allow for comparison between the cities. Correlations between percent length of hotspots and per capita GDP (Fig. 3a), road density (Fig. 3b) and the VSL (Fig. 3c) were drawn for each city, reflecting the influence of varied levels of economic development of the different countries (Levinson, 2002). Linear, quadratic, cubic and exponential regression models have been found to describe the relationship between air pollution and socio-economic factors (Luo et al. 2014) as also observed in our case. Fig. 3a shows an opposite trend between percent length of hotspots and per capita GDP for each city, except for CAN. Low-income (US$ <953) African cities (ADD and BLZ) showed the highest percent length of hotspots. This trend starts to decrease following a quadratic regression model, among the cities under study reaching the lowest for SAO (16%), which has the second highest GDP across all cities (US$ 5.9 k). CAN showed the highest GDP (US$ 13.4 k) as well as a high percent length of hotspots, which makes it an outlier. These findings are consistent with earlier studies that show an exponential decay between outdoor $PM_{2.5}$ concentration and GDP (Anenberg et al., 2019; Hasenkopf et al., 2016; Kumar et al., 2021). The percent length of hotspots showed an increasing trend with an increase in road density (Fig. 3b). This positive correlation, despite being weak, is as expected since road density is an indicator of the congestion of roads in a specific area, suggesting that high percent length of hotspots in cities may be due to high road densities. Finally, the benefits of avoided air pollution mortality are monetised using the VSL. VSL ranged from 0.058 (BLZ) to 1.695 (SAO) million US$ amongst the studied cities, where the percent length of hotspot shows a negative correlation with increase in VSL (Fig. 3c). This shows that cities with high VSL have lower percent length of hotspots, except for CAN. The above findings suggest

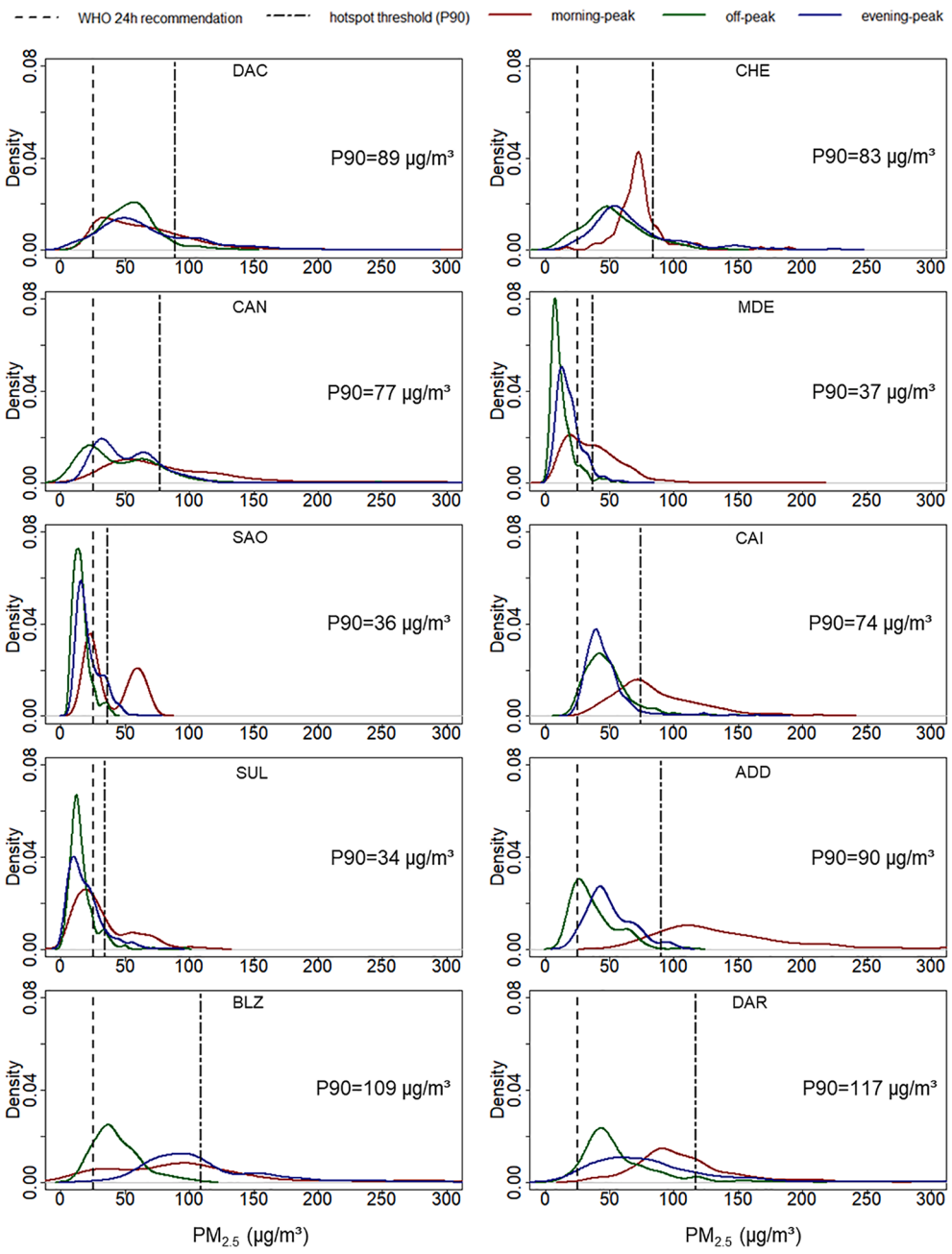

Fig. 1. Density plot of one-minute $PM_{2.5}$ concentration (µg m^{-3}) in all cities under windows-open car setting during morning and evening peak hours (red and blue lines, respectively) and off-peak hours (green line). The dotted lines represent the WHO $PM_{2.5}$ 24-hour mean guideline of 25 µg m^{-3} and the P90 value that varies for each city. (For interpretation of the references to colour in this figure legend, the reader is referred to the web version of this article.)

correlations between socio-economic factors and conditions of environmental degradation, expressed here as percent length of hotspots in which car commuters are exposed to excess $PM_{2.5}$ concentrations above daily WHO limits in each city. Presenting this dynamic put matters in perspective for governmental bodies, enabling them to plan urban mobility strategies in cities with consideration to hotspot areas, as it reflects on the local economy. For example, Xie et al. (2016) reported that without mitigation, $PM_{2.5}$ pollution will lead to ~2% GDP loss in China in 2030. Furthermore, scatterplots explored the relationship between hotspot parameters (such as percentage inhaled $PM_{2.5}$ and the ratio of hotspot to free-flow $PM_{2.5}$) and socio-economic factors (including city-specific per capita GDP, road density and VSL) (SI Fig. S6). An increase in the ratio of hotspot to free-flow $PM_{2.5}$ is observed for higher city-specific per capita GDP and VSL values (SI Figs. S6d and S6e). A higher ratio of hotspot to free-flow $PM_{2.5}$ (>3) was seen for cities with relatively higher GDP such as CAN, SAO and MDE. Such information could benefit cities in addressing the issue of higher congestion zones on frequently traveled routes, such as those followed in this study. Moreover, higher inhaled $PM_{2.5}$ doses are associated with higher road density (Fig. S6a), which is expected due to traffic congestion. Unfortunately, Fig. S6b, c and f did not exhibit strong trends to draw meaningful observations. We believe that mapping pollution parameters against socio-economic parameters on a global scale would provide meaningful trends that would allow cities to understand local pollution drivers and share best practices. However, due to data availability constraints, this study has only provided preliminary concepts that can be built on in future studies

Table 4
Descriptive statistics of $PM_{2.5}$ concentrations during free-flow and hotspot distances under windows-open settings for each city. SE and STD refer to standard error of mean, and standard deviation, respectively.

	$PM_{2.5}$ during free-flow (<90 percentile) (μg m^{-3})				$PM_{2.5}$ at hotspots distances (>90 percentile) (μg m^{-3})			
Cities	Median	Mean	SE	STD	Median	Mean	SE	STD
DAC	49.3	49.9	0.4	19.2	110.7	121.3	1.1	30.6
CHE	58.2	56.0	1.0	16.5	103.8	112.4	4.0	30.4
CAN	41.6	43.2	0.8	18.2	105.4	149.3	7.9	103.7
MDE	14.7	16.3	0.2	8.4	50.5	55.0	1.0	17.6
SAO	17.6	18.7	0.2	6.9	56.6	54.5	0.6	9.9
CAI	44.1	45.8	0.4	12.3	97.8	105.5	1.8	28.9
SUL	15.0	15.8	0.2	7.5	52.5	55.1	1.2	17.1
ADD	40.8	43.5	1.1	17.8	126.0	142.8	4.6	47.0
BLZ	60.4	61.2	1.7	28.6	141.7	164.3	6.7	65.2
DAR	63.5	65.5	0.8	26.0	145.1	158.4	3.4	46.6

3.3. Fuel pricing and exposure levels

Fig. 4a–d shows fuel prices versus $PM_{2.5}$ exposure levels and inhaled doses of car commuters under the windows-open setting. Fig. 4a and b allow categorising cities into three groups. Group 1 (MDE, SAO and SUL) has relatively low fuel prices and the lowest $PM_{2.5}$ concentrations, defying the expectation that lower fuel prices would encourage traffic and hence increase pollution. The number of cars per inhabitant (indicated by bubble sizes in Fig. 4a) are also low, moderate and high for SUL, MDE and SAO, respectively, showing no trend amongst this group. Furthermore, average speeds (indicated by bubble sizes in Fig. 4b) are relatively low for MDE and SAO and high for SUL; again showing no trend. Low exposure level in MDE and SAO are independent of low fuel prices, high car reliance and low car speeds, and therefore could be due to more green areas around the route (Kumar et al., 2021), usage of different fuel types (Ramírez et al., 2019) and less hotspots as discussed in Section 3.1. For example, Brazil has adopted the use of biofuel ethanol since the 1980s, and currently, all passenger cars can choose between using 100% ethanol or a 27% ethanol +73% gasoline mixture, thus contributing to a reduction of PM concentrations in the last decade in SAO (Andrade et al., 2017). As for SUL, low $PM_{2.5}$ concentrations could be due to flowing traffic, indicated by high speed, and a low number of cars per inhabitant. Group 2 (CAI and ADD; Fig. 4a–b) exhibits the lowest fuel prices, high $PM_{2.5}$ concentrations, a relatively high number of cars per inhabitant and moderately lower car speeds. This group follows the expected trend where low fuel prices encourage car ownership and in turn high congestion and high pollution levels as anticipated by several policy reports (Delsalle, 2002; Levin et al., 2017; Rouhani, 2014; Litman, 2011). Group 3 (DAC, CHE, CAN, BLZ and DAR; Fig. 4a-b) showed high $PM_{2.5}$ concentrations despite the relatively high fuel prices. This could be due to increased car reliance shown by large bubble sizes in all cities, except for DAC (Fig. 4a), thus indicating that despite the high fuel prices, commuters still resort to car transport, possibly due to the lack of alternative transport modes. High $PM_{2.5}$ concentrations in DAC could also be due to complex road infrastructures, faulty traffic signalling systems and narrow roads resulting in congestion despite the limited number of cars per inhabitant (Mahmud et al., 2012). Furthermore, Fig. 4b shows relatively low speeds for all cities of this group, except CAN, indicating congestion. Despite the flowing traffic in CAN, exposure is high due to economic advancement rates that surpass environmental control efforts (Managi and Kaneko, 2006; Shi et al., 2011). Overall, it can be deduced that controlling fuel price cannot stand as an effective policy measure on its own in controlling air pollution as fuel cost is not the only component of transport cost (Delsalle, 2002). Furthermore, $PM_{2.5}$ levels vary in response to other factors in addition to cost-controlled congestion levels including, urban infrastructure and design, transport alternatives and green spaces.

To further understand the impact of fuel price on pollution levels, Fig. 4c and d combine cities into groups 1 and 2. Group 1 includes cities that have fuel prices less than US$ 0.75 per litre and experience $PM_{2.5}$ inhaled doses of less than 2 μg km^{-1} travelled. BLZ, however, has slightly higher inhaled doses. Group 2 has cities that have more expensive fuel prices and higher inhaled doses with DAR seen as exceptionally high owing to its high $PM_{2.5}$ exposure concentrations and long trip durations. Variations in the number of cars per inhabitant and average speeds indicated by bubble sizes in Fig. 4c and d, respectively, do not justify pollution variations in response to fuel cost variations. This representation further confirms pollution levels inhaled by car commuters are to an extent independent to fuel price variations. Fuel price control measures could mitigate congestion and transport pollution; however, they cannot stand alone as effective measures since they are not the only factor in transport cost.

3.4. Health and economic impact

3.4.1. Heath burden

Table 6 provides a summary of *HB* in terms of number of deaths per year and the corresponding economic losses for each city. The annual deaths within the car commuters population resulting from $PM_{2.5}$ exposure during windows-open vary between MP, OP and EP. The highest number of deaths occurred as a result of MP exposure for all cities, except for DAR. This is due to the highest $PM_{2.5}$ concentrations

Table 5
Mean length of segments of free-flow and hotspot driving conditions in each city with average time spent in those sections of study route. ID_t (μg $kg^{-1}h^{-1}$) and ID_d (μg km^{-1}) for traffic hotspots and free-flow for each city.

Cities	Mean length (km)[a]		Average time spent at (min)[b]		Potential inhaled dose per unit time basis (ID_t; μg $kg^{-1}h^{-1}$)		Potential inhaled dose per distance driven (ID_d; μg km^{-1})	
	Hotspots	Free-flow	Hotspots	Free-flow	Hotspots	Free-flow	Hotspots	Free-flow
DAC	6.59	25.81	32.24	126.16	1.32	0.54	8.09	3.33
CHE	2.42	11.28	5.84	27.26	1.22	0.61	3.71	1.85
CAN	6.32	18.28	8.76	25.34	1.62	0.47	2.82	0.82
MDE	2.80	13.80	8.83	43.47	0.60	0.18	2.36	0.70
SAO	2.00	10.60	7.83	41.57	0.59	0.20	2.92	1.00
CAI	3.22	12.98	8.35	33.65	1.15	0.50	3.73	1.62
SUL	5.61	27.49	10.87	53.33	0.60	0.17	1.46	0.42
ADD	3.00	7.60	10.29	26.01	1.55	0.47	6.67	2.03
BLZ	2.71	8.19	7.26	21.94	1.78	0.66	6.00	2.24
DAR	3.37	16.83	22.24	111.06	1.72	0.71	14.26	5.90

[a] Mean length of hotspots ($PM_{2.5}$ concentration≥P90) and free-flow ($PM_{2.5}$ concentration≤P90) are calculated from the average time spent in corresponding traffic flow conditions and average speed of the car during the journey as described in Section 2.3.

[b] Average time spent in hotspots and free-flow represent the time corresponding to the mean number of data points (one-minute averaged) in each flow condition.

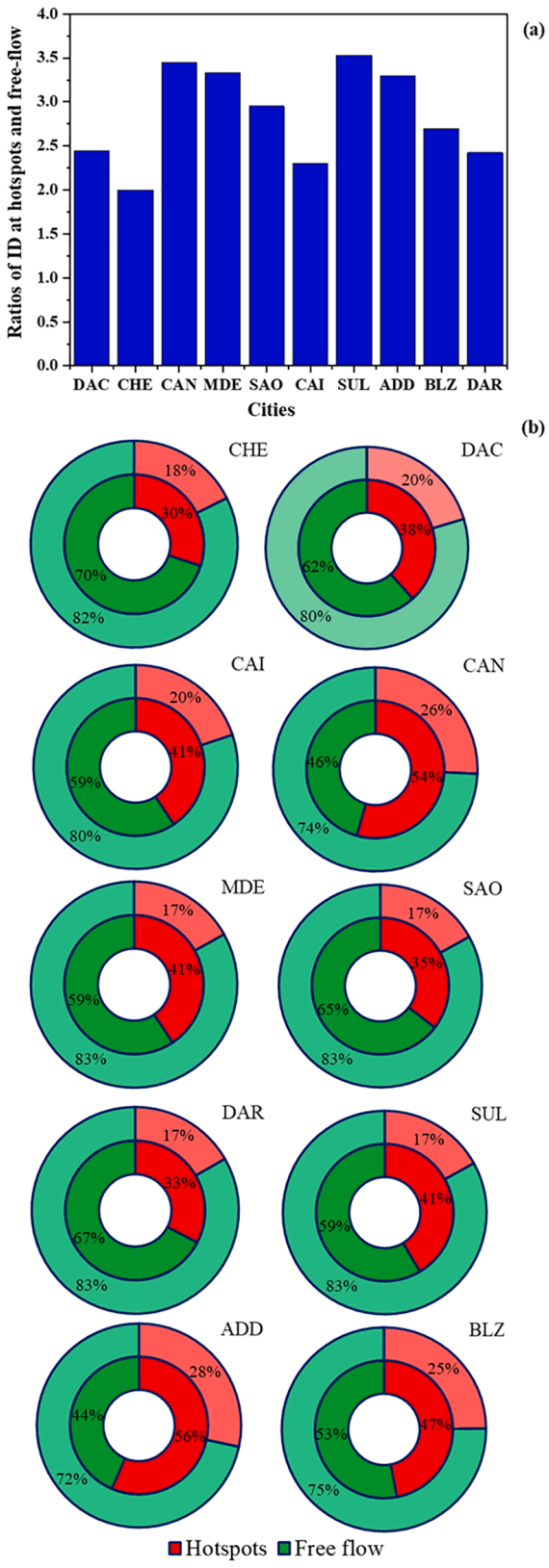

Fig. 2. (a) Bar Plots showing ratios of traffic hotspots/free-flow conditions for ID_d (blue) in studied cities. (b) Pie charts showing the percentage of time spent (outer circle) and inhaled $PM_{2.5}$ doses (inner circle) at traffic hotspots and during free-flow conditions. The colours red and green denote traffic hotspots and free-flow conditions, respectively. (For interpretation of the references to colour in this figure legend, the reader is referred to the web version of this article.)

during MP compared with OP and EP for all cities (Table 2). The highest concentrations during MP hours are associated with higher vehicle emissions during these periods in most cities, together with unfavorable pollutant dispersion conditions caused by the usually lower planetary boundary layer during mornings compared with mid-day (Quan et al., 2013). This is despite the fact that car commuters spend slightly more time in traffic during EP than MP (Table S5), indicating that pollutant concentrations are a higher contributor to *HB* than the time spent in traffic. However, for DAR, MP concentrations are higher than EP but the time spent in traffic during EP is 1.7-times that spent during MP causing deaths to be slightly higher during EP. DAR has the highest absolute number of deaths per year of 64 (95% CI: 60–69), followed by ADD 24 (95% CI: 22–27), CAN 16 (95% CI: 13–19) and CAI 15 (95% CI: 14–17) as shown in Fig. 4e and spatially in Fig. S7a. These cities, spreaded across all studied continents except Latin America (Fig. S7a), experience the highest in-car $PM_{2.5}$ concentrations and thereby lead to a higher number of premature deaths. However, other cities have high average $PM_{2.5}$ concentrations but fewer deaths per year, e.g. DAC: 6 (95% CI: 5–6), CHE: 9 (95% CI: 8–10) and BLZ: 2 (95% CI: 2–2); Fig. 4e. The average $PM_{2.5}$ concentrations in DAR and BLZ is 81.6 ± 39.3 and 82.9 ± 44.0 μgm^{-3}, respectively, which indicates that $PM_{2.5}$ concentrations are not the only variables driving the absolute number of annual premature deaths in each city. It is also driven by the exposed population, which is a product of the number of cars in a city and the car occupancy, which is evidently high for DAR, ADD, CAN and CAI and is in the order of 2–3 million people. Conversely, the exposed population of BLZ is almost 200,000 people which is only ~7% of that of DAR. Furthermore, the exposed population in SAO is ~8 million, but its average in-car $PM_{2.5}$ concentration is 25.6 ± 11.7 μgm^{-3}, resulting in 8 (95% CI: 7–9) deaths per year that is almost equal to those in CHE, which experiences an average $PM_{2.5}$ concentration of 65.2 ± 26.7 μgm^{-3} (2.5-times that of SAO) but has 15% of SAO's exposed population. Fig. 4f shows the national *HB* per year against average $PM_{2.5}$ concentrations. The baseline mortality is another variable used to derive HB. However, all mortality caused across cities varied within a limited range of around an average of 589.6 (95% CI: 531.2–648.1) deaths per 100,000 (Table 3) and, therefore, was not a major driver in reflecting *HB* variations between cities. This shows that the number of premature deaths experienced among cities is largely dependent on the exposure to pollution as well as car reliance in a city. This indicates the importance of accounting for both the pollution levels and the choice of transport mode in addressing the issue of commuter exposure.

Table 6 also shows the premature annual deaths resulting in the car commuting population under the windows-closed and recirculation-on scenarios to compare with the windows-open setting, which is discussed further in Section S3 and Fig. S8. The number of deaths per year resulting from recirculation varies between 0 and 2 for most cities except DAR owing to the low $PM_{2.5}$ concentrations experienced by car commuters who have windows-closed and recirculation on. This further proves the impact of car settings on $PM_{2.5}$ concentrations and in turn, the national health burden.

The discussion thus far has focused on the absolute number of deaths per year for each city. However, deaths are typically discussed as per 100,000 to provide for a normalised comparison as summarised in Table 6. This analysis eliminates the impact of variations in exposed population variations where DAR showed the highest deaths per 100,000 of car commuting population per year of 2.46 (95% CI: 2.28–2.63), followed by BLZ 1.11 (95% CI: 0.97–1.26) and DAC at 1.10 (95% CI: 1.05–1.15), which had a less absolute number of deaths despite the high $PM_{2.5}$ levels. ADD, CHE, CAI and CAN experienced air pollution levels of 0.88 (95% CI: 0.79–0.97), 0.71 (95% CI: 0.63–0.8), 0.51 (95% CI: 0.48–0.55) and 0.5 (95% CI: 0.41–0.59) deaths per 100,000 of car commuting population/year, respectively. MED, SAO and SUL have modest deaths due to considerably low $PM_{2.5}$ levels. Table 6 lists the deaths per 100,000 resulting from exposure to ambient $PM_{2.5}$ pollution reported by GBD (GBD, 2019). These death rates have been adapted for

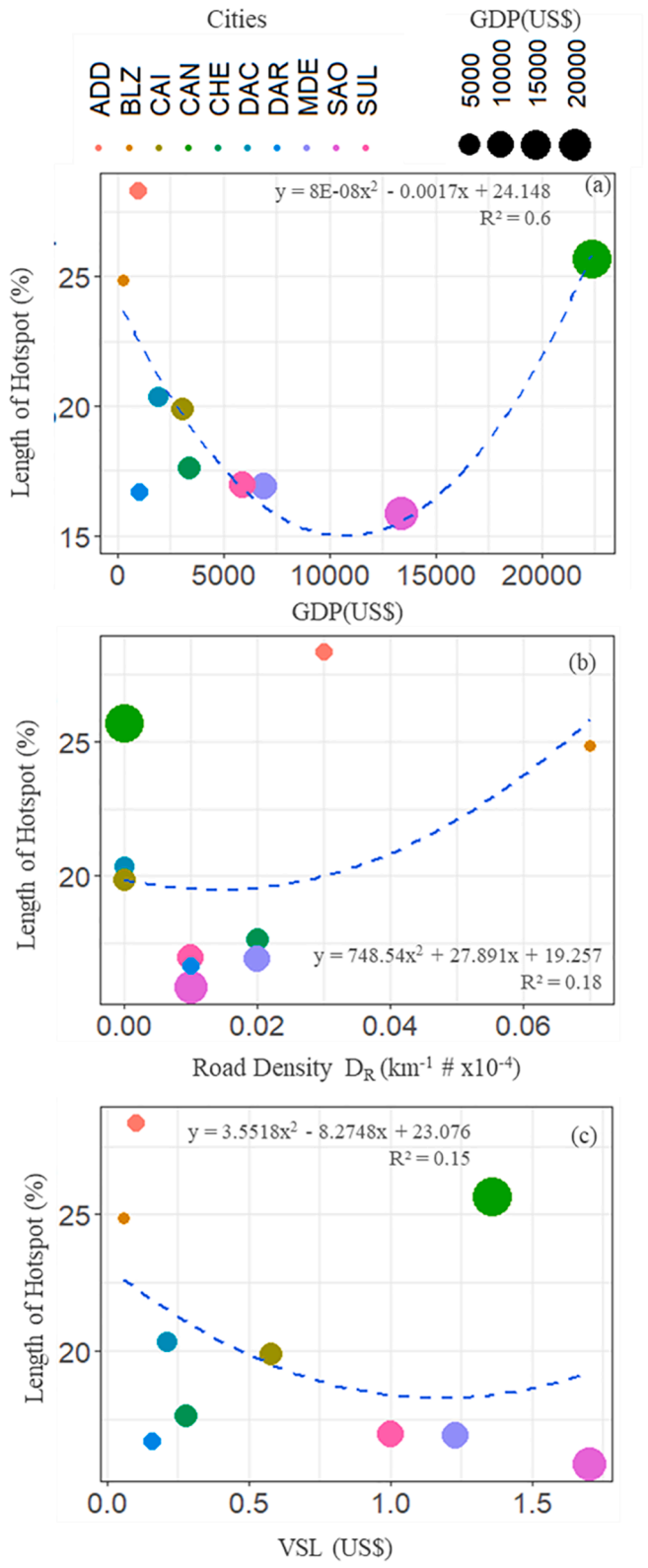

Fig. 3. Scatter plots showing relationships between percent length of hotspots versus (a) city-specific per capita GDP, (b) road density, and (c) VSL. The dotted line are drawn to simply visualise a trend. Size of the bubble points vary with respect to city-specific per capita GDP.

the car commuting population size derived for each city in Table 3 to enable comparison with the absolute annual deaths derived from our analysis. Fig. 4g shows the annual deaths resulting from in-car $PM_{2.5}$ exposure as a percentage of the total annual deaths within the car commuting population as a result of exposure to ambient $PM_{2.5}$ pollution. The percentage of car exposure deaths varies between 0 and 2% for most cities, which signifies that deaths caused by personal exposure to $PM_{2.5}$ in-car commutes are a small portion of the overall ambient $PM_{2.5}$ pollution which is caused by more factors than traffic pollution, such as industrial pollution. However, for the African cities (ADD, BLZ and DAR), the percentages are higher between 10 and 22%, showing that personal exposure to in-car $PM_{2.5}$ has a larger representation in terms of deaths per year due to the overall ambient $PM_{2.5}$ exposure. This is due to both the high in-car $PM_{2.5}$ concentrations as well as the smaller number of deaths per 100,000 caused by ambient $PM_{2.5}$ pollution reported by GBD (Table 6) in African cities compared to other cities. Overall, this analysis has allowed for translating pollution concentrations into associated premature deaths, which has provided a real-world dimension to scientific data, making it more relatable to policymakers and commuters.

3.4.2. *Economic loss*

To further quantify the losses felt by each city, *EL* for each city caused by short-term $PM_{2.5}$ exposure is calculated as a factor of the country's VSL in addition to pollution levels. Fig. 4h depicts GDP per capita versus national economic losses incurred by exposure to high $PM_{2.5}$ levels during car commutes showing that lower GDP is associated with higher economic losses caused by air pollution for most cities. This indicates a socioeconomic discrepancy which has been globally acknowledged where air pollution is more evident in developing countries (UNEP, 2019). CAN and SAO are outliers having higher GDP per capita and high economic losses. Both cities are located in opposite continents (Fig. S7b). For CAN, it is due to increased pollution exposure levels caused by economic advancement occurring at the expense of compromised environmental efforts (Managi and Kaneko, 2006; Shi et al., 2011). High EL is experienced by SAO despite the low $PM_{2.5}$ levels due to the combination of the relatively large proportion of the population using cars (37%) and to have the highest VSL amongst the group of considered cities (Table 3). MDE and SUL have modest *EL* as the observed $PM_{2.5}$ exposure concentrations did not exceed threshold concentrations. Overall, *HB* and *EL* are primarily dependent on pollution exposure levels; however, other factors such as the number of cars per city, car occupancy and national VSL play an important role in such metrics. This analysis reinforces the global nature of air pollution impact as a common issue that costs lives in all cities around the world regardless of the amount of EL incurred.

4. Conclusions and future outlook

We have presented an assessment of the trend between exposure levels, hotspots and socioeconomic indicators such as fuel prices, city-specific GDP, health burden and economic losses resulting from exposure to in-car $PM_{2.5}$ concentrations in ten cities across four continents (Asia, Latin America, Middle-East, and Africa). The following key conclusions are drawn:

- Irrespective of the cities, a relatively short time spent at hotspots contributed to a significant portion of total inhaled air pollution doses during a car commute. For example, the mean time spent in the car at hotspots in CAN and ADD accounted for only about 26–28% of the total time spent on each route, but corresponded to much higher (54–56%) of the total inhaled doses during a trip.
- An increase in the per cent length of the hotspot was observed with an increase in road density. The per cent length of hotspot shows a negative correlation with an increase in GDP and VSL among cities, except the CAN.

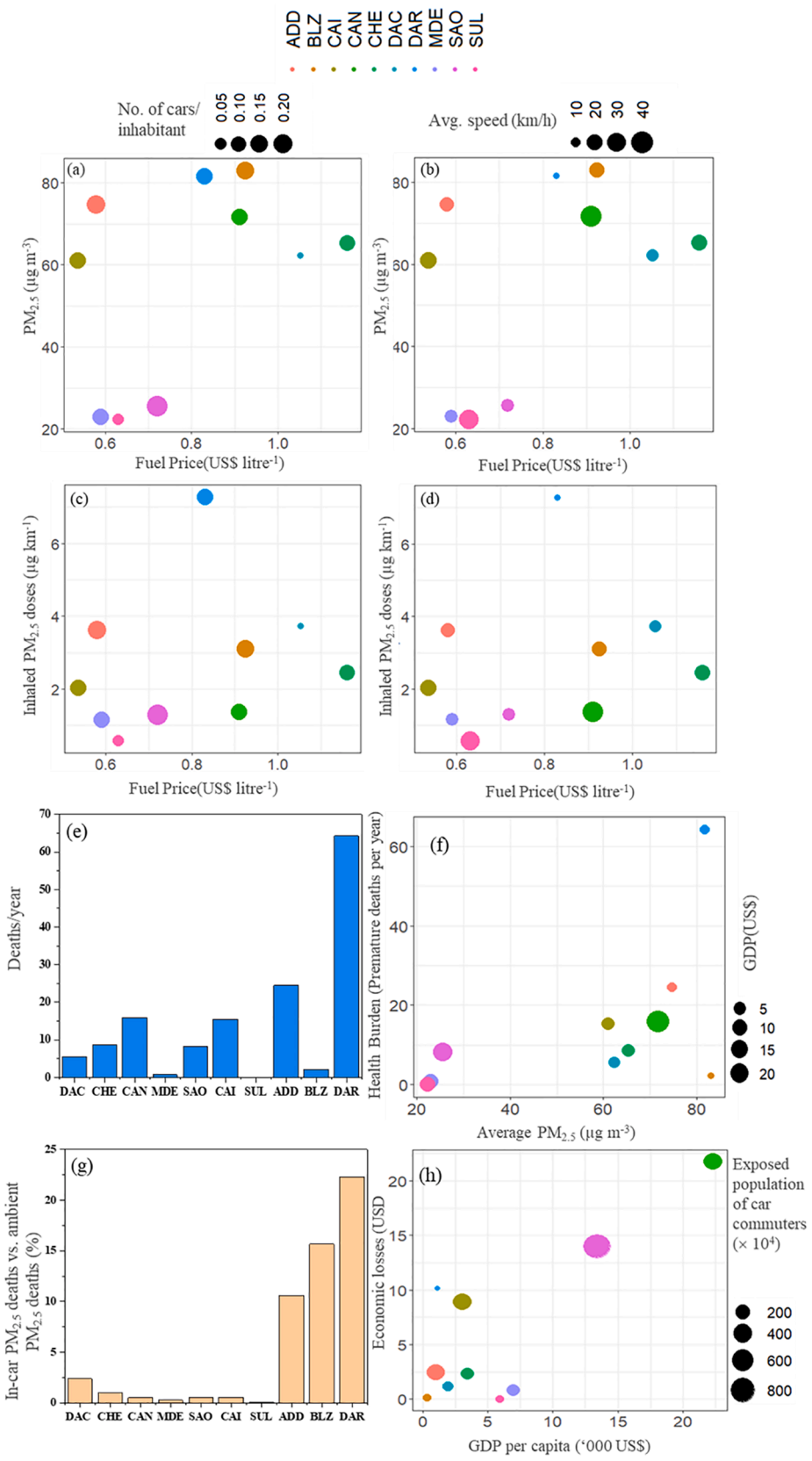

Fig. 4. Scatter plots of the relationship between average $PM_{2.5}$ concentrations and fuel price showing, via size of bubbles, (a) number of cars per inhabitant and (b) average car speeds. Likewise, (c) and (d) show the relationship between inhaled dose per unit distance driven and fuel price with (c) number of cars per inhabitant and (d) average car speeds via the size of the bubbles, respectively. Further plots show the relationship between (e) average premature annual deaths with CI-95% resulting from in-car $PM_{2.5}$ exposure; (f) average $PM_{2.5}$ concentrations and the national *HB* per year; (g) the percentage of deaths per year resulting from $PM_{2.5}$ car exposure out of deaths per year resulting from ambient PM pollution - both numbers referenced to the car commuters population for each city; and (h) city-specific per capita GDP and national EL owing to the in-car exposure to $PM_{2.5}$.

- Only CAI and ADD follow the expected trend of high pollution levels and low fuel costs. MDE, SAO and SUL have low pollution levels despite low fuel prices, and the rest of the cities studied experience high pollution levels despite high fuel prices. $PM_{2.5}$ exposure has proven to be independent of fuel prices indicating that controlling fuel price cannot stand as an effective policy measure on its own in mitigating air pollution since there are other factors that contribute to transport costs and commuter transport choices.
- The highest health burden was experienced by DAR, BLZ and DAC where 2.46 (95% CI: 2.28–2.63), 1.11 (95% CI: 0.97–1.26) and 1.10 (95% CI: 1.05–1.15) deaths per 100,000 of the car commuting population occurred per year, respectively, due to having the highest $PM_{2.5}$ car exposure concentrations amongst all cities of 81.6 ± 39.3, 82.9 ± 44.0 and 62.3 ± 32.0μgm^{-3}, respectively. However, MDE, SAO and SUL experienced low $PM_{2.5}$ levels of 23 ± 13.7, 25.6 ± 11.7 and 22.4 ± 15.0 μg m^{-3}, respectively, and hence experienced negligible health burden of 0.07 (95% CI: 0.06–0.08), 0.1 (95% CI: 0.09–0.12) and 0.02 (95% CI: 0.02–0.03) deaths per 100,000 of the car commuting population per year, respectively.
- The economic losses related to the health burden caused by $PM_{2.5}$ car exposure was measured against GDP per capita showing that lower GDP is associated with higher economic losses caused by in-car $PM_{2.5}$ exposure for most cities, increasing to 8.9 and 10.2 million US$ per year for CAI and DAR, respectively. This indicates a socioeconomic discrepancy where air pollution and its health and economic costs are more felt in developing countries. However, CAN and SAO incurs the highest economic losses of 21.8 and 14 million US$ per year due to high VSL for these countries.
- Clear correlation showing increases in health burden and economic losses were observed with hotspot parameters highlighting the positive impact that would be achieved if hotspots were tackled as major problem areas within an urban environment.

An assessment of in-car $PM_{2.5}$ health burden, economic cost and potential inhaled doses at hotspots have been estimated for ten cities. Similar studies in different modes of transport such as trains and buses considering gaseous pollutants are recommended to build a similar database for a more holistic assessment of the impact of transport emissions. This work would be further enhanced if other factors that contribute to transport costs are taken into consideration and assessed for their effectiveness as pollution mitigation measures. Further, the methodology adopted to calculate health burden and economic loss would be more accurate if city-specific information was available. This includes disease response parameters that are directly linked to $PM_{2.5}$ as well as economic metrics that would more thoroughly assess the cost of morbidity associated with $PM_{2.5}$ in addition to m ortality. Temporal variations introduced by 24-hr exposure–response coefficients used for this study can be more thoroughly addressed (e.g. Zheng et al., 2021), which was not feasible in this work given the limitations posed by the data availability and complexity (Section 2.5). Hence, health burden and economic losses results (Section 3.4) should be considered as indicative estimates and interpreted cautiously. Overall, this work has provided a preliminary basis for better employing short-term air pollution exposure data to set the ground for more detailed analysis in cities elsewhere.

CRediT authorship contribution statement

Prashant Kumar: Conceptualization, Funding acquisition, Resources, Methodology, Supervision, Project administration, Writing - original draft, Writing - review & editing. **Sarkawt Hama:** Writing - original draft, Data curation, Visualization, Validation, Writing - review & editing. **Rana Alaa Abbass:** Formal analysis, Data curation, Writing - original draft, Investigation, Writing - original draft, Writing - review & editing. **Thiago Nogueira:** Writing - original draft, Investigation, Validation, Writing - review & editing. **Veronika S. Brand:** Writing - original draft, Investigation, Validation, Writing - review & editing. **K.V. Abhijith:** Formal analysis, Data curation, Writing - original draft, Investigation, Writing - review & editing. **Maria Fatima Andrade:** Writing - review & editing. **Araya Asfaw:** Writing - review & editing. **Kosar Hama Aziz:** Writing - review & editing. **Shi-Jie Cao:** Investigation, Writing - review & editing. **Ahmed El-Gendy:** Writing - review & editing. **Mukesh Khare:** Writing - review & editing. **Adamson S. Muula:** Writing - review & editing. **S.M. Shiva Nagendra:** Writing - review & editing. **Aiwerasia Vera Ngowi:** Writing - review & editing. **Khalid Omer:** Writing - review & editing. **Yris Olaya:** Writing - review & editing. **Abdus Salam:** Writing - review & editing.

Declaration of Competing Interest

The authors declare that they have no known competing financial

Table 6
HB indicates the absolute number of deaths within the car commuting population owing to hourly exposure to high $PM_{2.5}$ levels under windows-open setting during MP, OP, EP and the sum of all three-time segments resulting from all commutes within one year. Numbers are represented as averages with a CI of 95% of (lower–upper). The corresponding annual *EL* are listed based on the total absolute number of deaths. *HB* is also listed for the recirculation setting based on data in Table S5. The total *HB* for windows-open is calculated per 100,000 people of the car commuting population to be compared with the deaths per 100,000 in 2019 reported by GBD resulting from ambient PM pollution.

City	*HB* for different time segments (deaths/year)[a]			Total *HB* (deaths/year)[a]	*EL* ($million/year)[a]	Total *HB* for recirculation setting (deaths/year)	*HB* (deaths per 100,000 car commuters/year)[a]	GBD of ambient PM pollution (deaths per 100,000)[b]
	MP	OP	EP					
DAC	2 (2–2)	1 (1–1)	3 (2–3)	6 (5–6)	1.1 (1.1–1.2)	0 (0–0)	1.10 (1.05–1.15)	46.45 (30.33–64.34)
CHE	3 (3–3)	2 (1–2)	4 (3–4)	9 (8–10)	2.4 (2.1–2.6)	1 (1–2)	0.71 (0.63–0.8)	70.44 (55.37–85.7)
CAN	9 (8–11)	3 (3–4)	4 (3–4)	16 (13–19)	21.8 (17.8–25.7)	2 (2–2)	0.5 (0.41–0.59)	100.09 (82.03–119.03)
MDE	1 (1–1)	0 (0–0)	0 (0–0)	1 (1–1)	0.9 (0.7–1.0)	0 (0–0)	0.07 (0.06–0.08)	27.28 (18.55–38.14)
SAO	8 (7–9)	0 (0–0)	0 (0–0)	8 (7–9)	14 (12.2–15.8)	0 (0–0)	0.1 (0.09–0.12)	20.11 (14.38–26.44)
CAI	7 (7–9)	4 (4–4)	4 (4–5)	15 (14–17)	8.9 (8.3–9.5)	2 (1–2)	0.51 (0.48–0.55)	91.41 (67.45–117.97)
SUL	0 (0–0)	0 (0–0)	0 (0–0)	0 (0–0)	0 (0–0.1)	0 (0–0)	0.02 (0.02–0.03)	60.25 (45.96–75.02)
ADD	18 (16–19)	3 (2–3)	4 (4–5)	24 (22–27)	2.5 (2.2–2.8)	1 (1–2)	0.88 (0.79–0.97)	8.32 (3.89–15.05)
BLZ	1 (1–1)	0 (0–0)	1 (1–1)	2 (2–2)	0.1 (0.1–0.1)	0 (0–0)	1.11 (0.97–1.26)	7.11 (3.22–13.47)
DAR	24 (23–26)	11 (10–12)	29 (27–32)	64 (60–69)	10.2 (9.4–10.9)	23 (21–26)	2.46 (2.28–2.63)	11.01 (5.84–18.38)

[a] Data is derived based on in-car $PM_{2.5}$ concentrations of windows-open setting.

[b] GBD (2019).

interests or personal relationships that could have appeared to influence the work reported in this paper.

Acknowledgements

This work was carried out under the framework of the Clean Air Engineering for Cities (CArE-Cities) project, which is funded by the University of Surrey's Research England funding under the Global Challenge Research Fund (GCRF) programme. MFA, TN and VSB acknowledge the São Paulo Research Foundation (FAPESP Grant no. 16/18438-0, 16/14501-0, and 2020/08505-8). TN and PK acknowledge the financial support received from the Institute of Advanced Studies at the University of Surrey. The authors thank Steve Manyozo, Shariful Islam, Farah Jeba, Simon Henry Mamuya, Jenny Martinez, Ming-Rui Meng and Lucas Cagnotto de Moraes for their help during the data collection of in-car $PM_{2.5}$ exposure in different cities.

Appendix A. Supplementary material

Supplementary data to this article can be found online at https://doi.org/10.1016/j.envint.2021.106688.

References

Abbass, R.A., Kumar, P., El-Gendy, A., 2020. Car users exposure to particulate matter and gaseous air pollutants in megacity Cairo. Sustain. Cities Soc. 56, 102090.
Abou-Ali, H., Thomas, A., 2011. Regulating Traffic to Reduce Air Pollution in Greater Cairo, Egypt. https://ideas.repec.org/p/erg/wpaper/664.html (accessed 10.09.2020).
AMVA, 2012. Encuesta origen destino de hogares para el Valle de Aburrá. Informe Final. https://www.medellin.gov.co/movilidad/jdownloads/Normas/TPM/Cuarto%20de%20Datos/informe_eod_hogares_2012.pdf (accessed 10.10.2020).
Abbass, R.A., Kumar, P., El-Gendy, A., 2021. Fine particulate matter exposure in four transport modes of Greater Cairo. Science of The Total Environment 148104.
Andrade, M.F., Kumar, P., Freitas, E.D., Ynoue, R.Y., Martins, J., Martins, L.D., Nogueira, T., Perez-Martinez, P., Miranda, R.M., Albuquerque, T., Gonçalves, F.L.T., Oyama, B., Zhang, Y., 2017. Air quality in the megacity of São Paulo: evolution over the last 30 years and future perspectives. Atmos. Environ. 159, 66–82.
Anenberg, S.C., Achakulwisut, P., Brauer, M., Moran, D., Apte, J.S., Henze, D.K., 2019. Particulate matter-attributable mortality and relationships with carbon dioxide in 250 urban areas worldwide. Sci. Rep. 9, 1–6.
Arif, A.T., Maschowski, C., Khanaqa, P., Garra, P., Garcia-Käufer, M., Wingert, N., Mersch-Sundermann, V., Gminski, R., Trouvé, G., Gieré, R., 2018. Characterisation and in vitro biological effects of ambient air PM_{10} from a rural, an industrial and an urban site in Sulaimani City, Iraq. Toxicol. Environ. Chem. 100, 373–394.
Azimi, P., Stephens, B., 2020. A framework for estimating the US mortality burden of fine particulate matter exposure attributable to indoor and outdoor microenvironments. J. Eposure Sci. Environ. Epidemiol. 30, 271–284.
Barnett, A.G., Knibbs, L.D., 2014. Higher fuel prices are associated with lower air pollution levels. Environ. Int. 66, 88–91.
Bauer, K., Bosker, T., Dirks, K.N., Behrens, P., 2018. The impact of seating location on black carbon exposure in public transit buses: implications for vulnerable groups. Transport. Res. Part D: Transp. Environ. 62, 577–583.
Betancourt, R.M., Galvis, B., Balachandran, S., Ramos-Bonilla, J.P., Sarmiento, O.L., Gallo-Murcia, S.M., Contreras, Y., 2017. Exposure to fine particulate, black carbon, and particle number concentration in transportation microenvironments. Atmos. Environ. 157, 135–145.
Betancourt, R.M., Galvis, B., Rincón-Riveros, J.M., Rincón-Caro, M.A., Rodriguez-Valencia, A., Sarmiento, O.L., 2019. Personal exposure to air pollutants in a Bus Rapid Transit System: impact of fleet age and emission standard. Atmos. Environ. 202, 117–127.
Bjorn, L., 2019. Arab Republic of Egypt: Cost of Environmental Degradation – Air and Water Pollution. The World Bank. https://openknowledge.worldbank.org/handle/10986/32513 (accessed 22.09.2020).
BRTA, 2018. Number of Registered Motor Vehicles in Dhaka. Bangladesh Road Transport Authority. https://brta.portal.gov.bd/sites/default/files/files/brta.portal.gov.bd/monthly_report/c6b00557_49aa_412d_b2e3_5b1409db3152/Dhaka%20Metro.pdf (accessed 10.10.2020).
Bigazzi, A.Y., Figliozzi, M.A., 2014. Review of urban bicyclists' intake and uptake of traffic-related air pollution. Transport Reviews 34 (2), 221–245.
Capentieri, M., Kumar, P., 2011. Ground-fixed and on-board measurements of nanoparticles in the wake of a moving vehicle. Atmos. Environ. 45, 5837–5852.
CAPMAS, 2017. Inventory of Licensed Vehicles for 2016. Cairo, Egypt: Central Agency for Public Mobilization and Statistics, No. 71-21315-2016. https://www.ceicdata.com/en/egypt/number-of-registered-vehicles-annual/no-of-registered-vehicles-cairo-public-sector (accessed 10.10.2020).
Carpentieri, M., Kumar, P., Robins, A., 2012. Wind tunnel measurements for dispersion modelling of vehicle wakes. Atmos. Environ. 62, 9–25.
Carslaw, D.C., Ropkins, K., 2012. openair – an R package for air quality data analysis. Environ. Modell. Software 27–28, 52–61.
Carvalho, A.M., Krecl, P., Targino, A.C., 2018. Variations in individuals' exposure to black carbon particles during their daily activities: a screening study in Brazil. Environ. Sci. Pollut. Res. 25, 18412–18423.
Castillo-Camacho, M.P., Tunarrosa-Grisales, I.C., Chacón-Rivera, L.M., Guevara-Luna, M. A., Belalcázar-Cerón, L.C., 2020. Personal exposure to $PM_{2.5}$ in the massive transport system of Bogotá and Medellín, Colombia. Asian J. Atmosp. Environ. 14, 210–224.
CEIC, 2016. Malawi Motor Vehicle Registered https://www.ceicdata.com/en/indicator/malawi/motor-vehicle-registered (accessed 10.10.2020).
CETESB, 2019. Qualidade do ar no estado de São Paulo 2018. https://cetesb.sp.gov.br/ar/publicacoes-relatorios/ (accessed 12.10.2020).
CPP, 2019. http://www.citypopulation.de/Iraq-Cities.html (accessed 01.10.2020).
Cox, W., 2019. Average Chinese car travels as much as American car, New Geography. https://www.newgeography.com/content/006420-average-chinese-car-travels-much-american-car (accessed 10.10.2020).
de Nazelle, A., Fruin, S., Westerdahl, D., Martinez, D., Ripoll, A., Kubesch, N., Nieuwenhuijsen, M., 2012. A travel mode comparison of commuters' exposures to air pollutants in Barcelona. Atmospheric Environment 59, 151–159.
Delsalle, J., 2002. The effects of fuel price changes on the transport sector and its emissions-simulations with TREMOVE (No. 172). Directorate General Economic and Financial Affairs (DG ECFIN). European Commission.
deSouza, P., Lu, R., Kinney, P., Zheng, S., 2021. Exposures to multiple air pollutants while commuting: evidence from Zhengzhou, China. Atmosp. Environ. 247, 118168.
Embiale, A., Zewge, F., Chandravanshi, B.S., Sahle-Demessie, E., 2019. Commuter exposure to particulate matters and total volatile organic compounds at roadsides in Addis Ababa, Ethiopia. Int. J. Environ. Sci. Technol. 16, 4761–4774.
EMT, 2019. Ethiopia Ministry of Transportation. http://motr.gov.et/ (accessed 20.10.2020).
Fann, N., Lamson, A.D., Anenberg, S.C., Wesson, K., Risley, D., Hubbell, B.J., 2012. Estimating the National Public Health Burden Associated with Exposure to Ambient PM2.5 and Ozone: U.S. Public Health Burden of PM2.5 and Ozone. Risk Analysis 32, 81–95.
Fantke, P., McKone, T.E., Tainio, M., Jolliet, O., Apte, J.S., Stylianou, K.S., Illner, N., Marshall, J.D., Choma, E.F., Evans, J.S., 2019. Global Effect Factors for Exposure to Fine Particulate Matter. Environmental Science & Technology 53, 6855–6868.
Fecht, D., Fischer, P., Fortunato, L., Hoek, G., de Hoogh, K., Marra, M., Kruize, H., Vienneau, D., Beelen, R., Hansell, A., 2015. Associations between air pollution and socioeconomic characteristics, ethnicity and age profile of neighbourhoods in England and the Netherlands. Environ. Pollut. 198, 201–210.
Farmer, P., 2020. Designing for Personal drone vehicle capability for Sao Paulo, Brazil. Chapman Taylor. https://www.chapmantaylor.com/insights/designing-for-personal-drone-vehicle-capability-for-sao-paulo-brazil (accessed 10.10.2020).
Fraser, S., Haworth, S., 2017. Malawi National Transport Master Plan. http://npc.mts.mw/wp-content/uploads/2020/07/National-Transport-Master-Plan1.pdf (accessed 10.10.2020).
GBD, 2019. Global Burden of Disease: All causes deaths per 100,000, Both sexes, All ages. https://vizhub.healthdata.org/gbd-compare/ (accessed 08.01.2021).
GBS, 2019. Guangzhou Bureau of Statistics. http://tjj.gz.gov.cn/gkmlpt/content/4/4071/post_4071297.html#226 (accessed 10.10.2020).
Giri, J.A., Karthikeyan, S., Raj, M.G., 2020. Effect of ambient concentration of carbon monoxide (CO) on the in-vehicle concentration of carbon monoxide in Chennai, India. Environ. Eng. Res. 26, 200165.
Goel, A., Kumar, P., 2015. Zone of influence for particle number concentrations at signalised traffic intersections. Atmos. Environ. 123, 25–38.
Goodman, A., Wilkinson, P., Stafford, M., Tonne, C., 2011. Characterising socioeconomic inequalities in exposure to air pollution: a comparison of socioeconomic markers and scales of measurement. Health Place 17, 767–774.
GPB, 2019. Transportation policy branch of Guangzhou policy bureau. https://www.yearbookchina.com/navipage-n3019121604000130.html (accessed 10.10.2020).
GPP, 2020. Global Petrol Prices. https://www.globalpetrolprices.com (accessed 10.11.2020).
Guiqin, G., Xingqin, X., Huayue, H., Yaqin, Y., Pengpeng, P., 2020. Assessment of the impact of $PM_{2.5}$ exposure on the daily mortality of circulatory system in Shijiazhuang, China. Atmosphere 11, 1018.
Hasenkopf, C.A., Adukpo, D.C., Brauer, M., Dewitt, H.L., Guttikunda, S., Ibrahim, A.I., Lodoisamba, D., Mutanyi, N., Olivares, G., Pant, P., Salmon, M., 2016. To combat air inequality, governments and researchers must open their data: commentary. Clean Air J. 26, 8–10.
Hassanien, M.A., Abdel-Latif, N.M., 2008. Polycyclic aromatic hydrocarbons in road dust over Greater Cairo, Egypt. J. Hazardous Mater. 151, 247–254.
HEI, 2010. Traffic-related Air Pollution: A Critical Review of the Literature on Emissions, Exposure, and Health Effects. Health Effects Institute, Boston, MA. https://www.healtheffects.org/publication/traffic-related-air-pollution-critical-review-literature-emissions-exposure-and-health (accessed 10.09.2020).
Hinds, W.C., 1999. Aerosol technology: properties, behavior, and measurement of airborne particles. John Wiley & Sons. ISBN: 978-0-471-19410-1, pp. 483.
Hossain, M.M., Majumder, A.K., Islam, M., Al Nayeem, A., 2019. Study on ambient particulate matter ($PM_{2.5}$) with different mode of transportation in Dhaka City, Bangladesh. Am. J. Pure Appl. Biosci. 1, 12–19.
Hu, J., Ying, Q., Wang, Y., Zhang, H., 2015. Characterising multi-pollutant air pollution in China: comparison of three air quality indices. Environ. Int. 84, 17–25.
Jackson, M.M., 2005. Roadside concentration of gaseous and particulate matter pollutants and risk assessment in Dar-Es-Salaam, Tanzania. Environ. Monit. Assess. 104, 385–407.

Ji, W., Zhao, B., 2015. Estimating mortality derived from indoor exposure to particles of outdoor origin. PLoS ONE 10 (4), e0124238.
Kiunsi, R.B., 2013. A review of traffic congestion in Dar es Salaam city from the physical planning perspective. J. Sustain. Develop. 6, 94.
Kloog, I., Ridgway, B., Koutrakis, P., Coull, B.A., Schwartz, J.D., 2013. Long- and short-term exposure to PM2.5 and mortality: using novel exposure models. Epidemiology 24, 555–561.
Kolluru, S.S.R., Patra, A.K., Sahu, S.P., 2018. A comparison of personal exposure to air pollutants in different travel modes on national highways in India. Sci. Total Environ. 619, 155–164.
KRSO, 2019. Kurdistan Regional Statistics Office. http://www.krso.net/ (accessed 30.09.2020).
Krzyzanowski, M., Kuna-Dibbert, B. Schneider, J., 2005. Health effects of transport-related air pollution. WHO Regional Office Europe, pp. 15–16 (accessed 30.10.2020).
Kumar, P., Garmory, A., Ketzel, M., Berkowicz, R., Britter, R., 2009. Comparative study of measured and modelled number concentrations of nanoparticles in an urban street canyon. Atmos. Environ. 43, 949–958.
Kumar, P., Patton, A.P., Durant, J.L., Frey, H.C., 2018. A review of factors impacting exposure to PM2.5, ultrafine particles and black carbon in Asian transport microenvironments. Atmos. Environ. 187, 301–316.
Kumar, P., Hama, S., Omidvarborna, H., Sharma, A., Sahani, J., Abhijith, K.V., Debele, S. E., Zavala-Reyes, J.C., Barwise, Y., Tiwari, A., 2020a. Temporary reduction in fine particulate matter due to 'anthropogenic emissions switch-off' during COVID-19 lockdown in Indian cities. Sustain. Cities Soc. 62, 102382.
Kumar, P., Goel, A., 2016. Concentration dynamics of coarse and fine particulate matter at and around signalised traffic intersections. Environmental Science: Processes & Impacts 18, 1220–1235.
Kumar, P., Hama, S., Nogueira, T., Abbass, R.A., Brand, V.S., de Fatima Andrade, M., Asfaw, A., Aziz, K.H., Cao, S.J., El-Gendy, A., Islam, S., 2021. In-car particulate matter exposure across ten global cities. Sci. Total Environ. 750, 141395.
Labib, S.M., Rahaman, Z., Patwary, M.S.H., 2014. Green Transport Planning For Dhaka City: Measures for Environment Friendly Transportation System. Undergraduate thesis Bangladesh University of Engineering and Technology. https://www.researchgate.net/publication/321962434 (10.10.2020).
Leavey, A., Reed, N., Patel, S., Bradley, K., Kulkarni, P., Biswas, P., 2017. Comparing on-road real-time simultaneous in-cabin and outdoor particulate and gaseous concentrations for a range of ventilation scenarios. Atmospheric Environment 166, 130–141.
Levin, M.W., Jafari, E., Shah, R., Boyles, S.D., 2017. Network-based model for predicting the effect of fuel price on transit ridership and greenhouse gas emissions. Int. J. Transp. Sci. Technol. 6, 272–286.
Levinson, A., 2002. The ups and downs of the environmental Kuznets curve. Recent Adv. Environ. Econ. 119–139.
Li, T., Guo, Y., Liu, Y., Wang, J., Wang, Q., Sun, Z., He, M.Z., Shi, X., 2019. Estimating mortality burden attributable to short-term PM2.5 exposure: a national observational study in China. Environ. Int. 125, 245–251.
Lin, H., Ma, W., Qiu, H., Wang, X., Trevathan, E., Yao, Z., Dong, G.-H., Vaughn, M.G., Qian, Z., Tian, L., 2017. Using daily excessive concentration hours to explore the short-term mortality effects of ambient PM2.5 in Hong Kong. Environ. Pollut. 229, 896–901.
Litman, T., 2011. Appropriate Response to Rising Fuel Prices. Victoria Transport Policy Institute. https://www.vtpi.org/fuelprice.pdf (20.12.2020).
Luo, Y., Chen, H., Peng, C., Yang, G., Yang, Y., Zhang, Y., 2014. Relationship between air pollutants and economic development of the provincial capital cities in China during the past decade. PLoS ONE 9, 104013.
Maciejewska, K., 2020. Short-term impact of PM2.5, PM10, and PMc on mortality and morbidity in the agglomeration of Warsaw, Poland. Air Qual. Atmos. Health 13, 659–672.
Mahmud, K., Gope, K., Chowdhury, S.M.R., 2012. Possible causes & solutions of traffic jam and their impact on the economy of Dhaka City. J. Manage. Sustain. 2, 112.
Maji, K.J., Ye, W.-F., Arora, M., Shiva Nagendra, S.M., 2018. $PM_{2.5}$-related health and economic loss assessment for 338 Chinese cities. Environ. Int. 121, 392–403.
Maji, K.J., Namdeo, A., Hoban, D., Bell, M., Goodman, P., Nagendra, S.S., Barnes, J., De Vito, L., Hayes, E., Longhurst, J., Kumar, R., 2021. Analysis of various transport modes to evaluate personal exposure to PM2. 5 pollution in Delhi. Atmos. Pollut. Res. 12, 417–431.
Managi, S., Kaneko, S., 2006. Economic growth and the environment in China: an empirical analysis of productivity. Int. J. Global Environ. Issues 6, 89.
Manojkumar, N., Monishraj, M., Srimuruganandam, B., 2021. Commuter exposure concentrations and inhalation doses in traffic and residential routes of Vellore city, India. Atmos. Pollut. Res. 12, 219–230.
Mapoma, H.W.T., Tenthani, C., Tsakama, M., Kosamu, I.B.M., 2014. Air quality assessment of carbon monoxide, nitrogen dioxide and sulfur dioxide levels in Blantyre, Malawi: a statistical approach to a stationary environmental monitoring station. Afr. J. Environ. Sci. Technol. 8, 330–343.
Mapoma, H.W.T., Xie, X., Zhang, L., Nyirenda, M.T., Maliro, A., Chimutu, D., 2016. Hydrochemical characteristics of rural community groundwater supply in Blantyre, southern Malawi. J. Afr. Earth Sc. 114, 192–202.
Matthaios, V.N., Kramer, L.J., Crilley, L.R., Sommariva, R., Pope, F.D., Bloss, W.J., 2020. Quantification of within-vehicle exposure to NOx and particles: variation with outside air quality, route choice and ventilation options. Atmos. Environ. 240, 117810.
Milner, J., Armstrong, B., Davies, M., Ridley, I., Chalabi, Z., Shrubsole, C., Vardoulakis, S., Wilkinson, P., 2017. An exposure-mortality relationship for residential indoor $PM_{2.5}$ exposure from outdoor sources. Climate 5, 66.
Morales, R., Galvis, B., Ramos-Bonilla, J.P., Balachandran, S., Sarmiento, O.L., Gallo-Murcia, S.M., Contreras, Y., 2017. Exposure to particulate pollution in transportation microenvironments in Bogotá, Colombia. J. Transp. Health 5, S59.
Nakat, Z., Herrera, S., Cherkaoui, Y., 2013. Cairo Traffic Congestion Study. World Bank. https://openknowledge.worldbank.org/handle/10986/18735 (accessed 10.02.2018).
Nansai, K., Tohno, S., Chatani, S., Kanemoto, K., Kurogi, M., Fujii, Y., Kagawa, S., Kondo, Y., Nagashima, F., Takayanagi, W., Lenzen, M., 2020. Affluent countries inflict inequitable mortality and economic loss on Asia via $PM_{2.5}$ emissions. Environ. Int. 134, 105238.
Nogueira, T., Dominutti, P.A., Vieira-Filho, M., Fornaro, A., Andrade, M.D.F., 2019. Evaluating atmospheric pollutants from urban buses under real-world conditions: implications of the main public transport mode in São Paulo, Brazil. Atmosphere 10, 108.
Nogueira, T., Kumar, P., Nardocci, A., de Fatima Andrade, M., 2020. Public health implications of particulate matter inside bus terminals in Sao Paulo, Brazil. Sci. Total Environ. 711, 135064.
Orellano, P., Reynoso, J., Quaranta, N., Bardach, A., Ciapponi, A., 2020. Short-term exposure to particulate matter (PM10 and PM2.5), nitrogen dioxide (NO2), and ozone (O3) and all-cause and cause-specific mortality: systematic review and meta-analysis. Environ. Int. 142, 105876.
Osra, 2016. Vehicle occupancy rates and trip purposes in Makkah during Ramadan and Hajj periods. Umm Al-Qura University, Saudi Arabia. https://www.researchgate.net/publication/311400958_VEHICLE_OCCUPANCY_RATES_AND_TRIP_PURPOSE_IN_MAKKAH_DURING_RAMADAN_AND_HAJJ_PERIODS (accessed 10.10.2020).
Parry, I.W.H., Timilsina, G.R., 2015. Demand-side instruments to reduce road transportation externalities in the greater Cairo Metropolitan Area. Int. J. Sustain. Transport. 9, 203–216.
Quan, J., Gao, Y., Zhang, Q., Tie, X., Cao, J., Han, S., Meng, J., Chen, P., Zhao, D., 2013. Evolution of planetary boundary layer under different weather conditions, and its impact on aerosol concentrations. Particuology 11, 34–40.
Rahman, A., Luo, C., Khan, M.H.R., Ke, J., Thilakanayaka, V., Kumar, S., 2019. Influence of atmospheric $PM_{2.5}$, PM_{10}, O_3, CO, NO_2, SO_2, and meteorological factors on the concentration of airborne pollen in Guangzhou, China. Atmos. Environ. 212, 290–304.
Raj, M.G., Karthikeyan, S., 2019. Effect of modes of transportation on commuters' exposure to fine particulate matter ($PM_{2.5}$) and nitrogen dioxide (NO_2) in Chennai, India. Environ. Eng. Res. 25, 898–907.
R Core Team, 2019. R: A language and environment for statistical computing. R Foundation for Statistical Computing, Vienna, Austria. https://www.R-project.org/.
Ramírez, J., Pachón, J.E., Casas, O.M., González, S.F., 2019. A new database of on-road vehicle emission factors for Colombia: a case study of Bogotá. CT & F-Ciencia Tecnología y Futuro 9, 73–82.
Richardson, E.A., Pearce, J., Tunstall, H., Mitchell, R., Shortt, N.K., 2013. Particulate air pollution and health inequalities: a Europe-wide ecological analysis. Int. J. Health Geograph. 12, 1–10.
Rivas, I., Kumar, P., Hagen-Zanker, A., de Fatima Andrade, M., Slovic, A.D., Pritchard, J. P., Geurs, K.T., 2017. Determinants of black carbon, particle mass and number concentrations in London transport microenvironments. Atmos. Environ. 161, 247–262.
Rouhani, O.M., 2014. Fuel consumption information: an alternative for congestion pricing? Road Transp. Res. 23, 52–64.
Sabapathy, A., Saksena, S., Flachsbart, P., 2015. Environmental justice in the context of commuters' exposure to CO and PM10 in Bangalore, India. J. Eposure Sci. Environ. Epidemiol. 25, 200–207.
Shang, Y., Sun, Z., Cao, J., Wang, X., Zhong, L., Bi, X., Li, H., Liu, W., Zhu, T., Huang, W., 2013. Systematic review of Chinese studies of short-term exposure to air pollution and daily mortality. Environ. Int. 54, 100–111.
Shen, F., Zhang, L., Jiang, L., Tang, M., Gai, X., Chen, M., Ge, X., 2020. Temporal variations of six ambient criteria air pollutants from 2015 to 2018, their spatial distributions, health risks and relationships with socioeconomic factors during 2018 in China. Environ. Int. 137, 105556.
Shen, J., Gao, Z., 2019. Commuter exposure to particulate matters in four common transportation modes in Nanjing. Build. Environ. 156, 156–170.
Shi, M., Ma, G., Shi, Y., 2011. How much real cost has China paid for its economic growth? Sustain. Sci. 6, 135–149.
SIGAIRE, 2017. Sistema integrado de gestión de la calidad del aire. Actualización inventario de emisiones atmosféricas del Valle de Aburra -ano 2016. https://www.metropol.gov.co/ambiental/calidad-del-aire/Documents/Inventario-de-emisiones/Inventario_FuentesM%C3%B3viles2016.pdf (accessed 10.10.2020).
STO, 2014. Sustainability Outlook. Vehicle Sharing - Exploring the Market in India. http://www.sustainabilityoutlook.in/content/vehicle-sharing-%E2%80%93-exploring-market-india-423821 (accessed 10.10.2020).
SYBI, 2017. Motor vehicles – Statistical Year Book India 2017. http://mospi.nic.in/statistical-year-book-india/2017/189 (accessed 10.10.2020).
Targino, A.C., Krecl, P., Cipoli, Y.A., Oukawa, G.Y., Monroy, D.A., 2020. Bus commuter exposure and the impact of switching from diesel to biodiesel for routes of complex urban geometry. Environ. Pollut. 263, 114601.
Targino, A.C., Rodrigues, M.V.C., Krecl, P., Cipoli, Y.A., Ribeiro, J.P.M., 2018. Commuter exposure to black carbon particles on diesel buses, on bicycles and on foot: a case study in a Brazilian city. Environ. Sci. Pollut. Res. 25, 1132–1146.
TMCRTE, 2009. The management of commercial road transport in Ethiopia. Private Sector Development Hub/Addis Ababa Chamber of Commerce and Sectoral Associations. file://surrey.ac.uk/personal/HS204/sh0073/downloads/15.pdf1abbyy.pdf. (accessed 10.10.2020).

Tong, R., Zhang, L., Yang, X., Zhou, P., Xu, S., 2019. Probabilistic health risk of volatile organic compounds (VOCs): comparison among different commuting modes in Guangzhou, China. Human Ecol. Risk Assess.: Int. J. 25, 637–658.
UN, 2018. United Nations The World's Cities in 2018-Data Booklet (ST/ESA/ SER.A/ 417). Department of Economic and Social Affairs, Population Division. https://www.un.org/en/events/citiesday/assets/pdf/the_worlds_cities_in_2018_data_booklet.pdf (accessed 10.11.2020).
UNEP, 2019. Air Pollution Hurts the Poorest Most. United Nations Environmental Program.
USEPA, 1992. United States Environmental Protection Agency Guidelines for Exposure Assessment. Risk Assess. Forum. http://ofmpub.epa.gov/eims/eimscomm.getfile?p_download_id=429103 (accessed 12.10.2020).
U.S. EPA, 2010. Quantitative Health Risk Assessment for Particulate Matter. U.S. Environmental Protection Agency, No. EPA-452/R-10-005. https://www3.epa.gov/ttn/naaqs/standards/pm/data/PM_RA_FINAL_June_2010.pdf (accessed 31.03.2021).
Viscusi, W.K., Masterman, C.J., 2017. Income elasticities and global values of a statistical life. J. Benefit-Cost Anal. 8, 226–250.
Vrijheid, M., Martinez, D., Aguilera, I., Ballester, F., Basterrechea, M., Esplugues, A., Guxens, M., Larrañaga, M., Lertxundi, A., Mendez, M., Murcia, M., 2012. socioeconomic status and exposure to multiple environmental pollutants during pregnancy: evidence for environmental inequity? J. Epidemiol. Commun. Health 66, 106–113.
WHO, 2006. Health risks of particulate matter from long-range transboundary air pollution. Bonn, Germany: European Centre for Environment and Health. https://www.euro.who.int/_data/assets/pdf_file/0006/78657/E88189.pdf (accessed 12.04.2021).
WHO, 2016. Goal 3: Ensure healthy lives and promote well-being for all at all ages – Indicator 3.9.1: Mortality rate attributed to household and ambient air pollution. World Health Organization. https://www.who.int/data/gho/data/indicators/indicator-details/GHO/ambient-and-household-air-pollution-attributable-death-rate-(per-100-000-population) (accessed 31.03.2021).
WHO, 2018. WHO Global urban ambient air pollution database (2018). Available at: https://www.who.int/airpollution/data/who-aap-database-may2016.xlsx?ua=1 (accessed 09.10.2020).
Xiang, J., Weschler, C.J., Wang, Q., Zhang, L., Mo, J., Ma, R., Zhang, J., Zhang, Y., 2019. Reducing indoor levels of 'outdoor $PM_{2.5}$' in urban China: impact on mortalities. Environ. Sci. Technol. 53, 3119–3127.
Xie, Y., Dai, H., Dong, H., Hanaoka, T., Masui, T., 2016. Economic impacts from PM2.5 pollution-related health effects in China: a provincial-level analysis. Environ. Sci. Technol. 50, 4836–4843.
Xu, W., Mai, G., Zhu, Q., Yu, Z., Liu, Y., 2016. Pollution exposure at bus commuter stations in Guangzhou, China. Int. J. Environ. Technol. Manage. 19, 103–119.
Yu, H., Stuart, A.L., 2016. Exposure and inequality for select urban air pollutants in the Tampa Bay area. Sci. Total Environ. 551, 474–483.
Zheng, J., Qiu, Z., Gao, H.O., Li, B., 2021. Commuter PM exposure and estimated life-expectancy loss across multiple transportation modes in Xi'an, China. Ecotoxicol. Environ. Safe. 214, 112117.
Gustafsson, M., Lindén, J., Tang, L., Forsberg, B., Orru, H., Åström, S., and Sjöberg, K., 2018. *Quantification of population exposure to NO_2, $PM_{2.5}$ and PM_{10} and estimated health impacts*. Stockholm, Sweden: IVL Swedish Environmental Research Institute, ISBN 978-91-88787-60-6 No. C 317. Available at: www.ivl.se (accessed 22.09.2020).
Chen, L.-J. and Lin, Y.-L., 2015. Does Air Pollution Respond to Petroleum Price? *International Journal of Applied Economics*, 12 (2), 104–125. Available at: https://www2.southeastern.edu/orgs/ijae/index_files/IJAE%20SEPT%202015%20CHEN%20LIN%2010-28-2015%20Air_Pollution_with_name_IJAE_20150224.pdf (accessed 21.09.2020).
TWB, 2018. The World Bank, 2018. Available at: https://data.worldbank.org/indicator/SP.DYN.CDRT.IN?end=2018&start=2018&view=map (accessed 10.10.2020).